CHALMERS
UNIVERSITY OF TECHNOLOGY

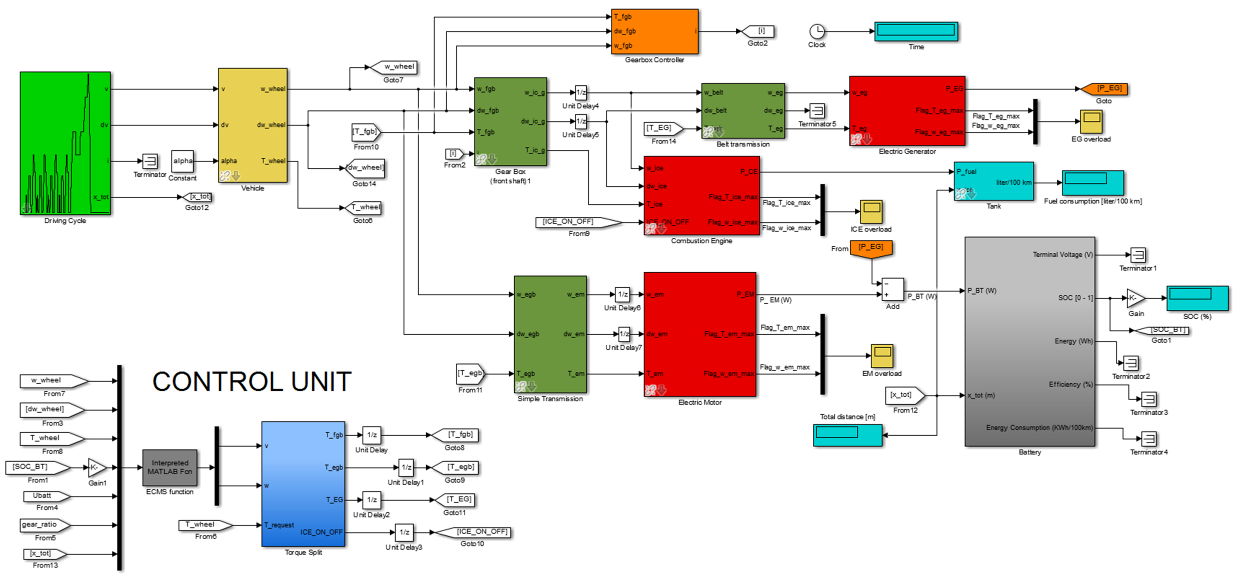


# Model Building and Energy Efficient Control of a Series-Parallel Plug-in Hybrid Electric Vehicle

*Master of Science Thesis*

DAVID CID FERNÁNDEZ

Department of Energy and Environment
*Division of Electric Power Engineering*
CHALMERS UNIVERSITY OF TECHNOLOGY
Göteborg, Sweden 2016

# Model Building and Energy Efficient Control of a Series-Parallel Plug-in Hybrid Electric Vehicle

DAVID CID FERNÁNDEZ

CHALMERS
UNIVERSITY OF TECHNOLOGY

Department of Energy and Environment
*Division of Electric Power Engineering*
Chalmers University of Technology
Göteborg, Sweden 2016

Model Building and Energy Efficient Control of a
Series-Parallel Plug-in Hybrid Electric Vehicle
DAVID CID FERNÁNDEZ

© DAVID CID FERNÁNDEZ, 2016.

Department of Energy and Environment
Division of Electric Power Engineering
Chalmers University of Technology
SE-412 96 Göteborg
Sweden
Telephone +46 (0)31-772 1000

Cover: Simulink model of a series-parallel PHEV

Chalmers Bibliotek, Reproservice
Göteborg, Sweden 2016

**Model Building and Energy Efficient Control of a Series-Parallel Plug-in Hybrid Electric Vehicle**
DAVID CID FERNÁNDEZ
Department of Energy and Environment
*Division of Electric Power Engineering*
Chalmers University of Technology

# Abstract

Among others, one of the European Union 2020 targets is to reduce the overall greenhouse gas emissions by at least 20% compared to 1990 levels. The ongoing introduction of electric and hybrid electric vehicles in the market seems to strongly support this objective. Hybrid electric vehicles (HEV) are those that combine an internal combustion engine with one or more electric machines. Series, parallel and series-parallel are the main HEV topologies. Plug-in hybrid electric vehicles are another topology which allows the battery to be charged using electricity from the grid. Since hybrid electric vehicles combine two or more energy sources, its control becomes really important but challenging at the same time. The role of the energy management strategy is to coordinate the power flow from the mechanical and electrical path. There are mainly two general energy management strategies: rule-based strategies and optimization-based algorithms.

In this thesis, a model of a series-parallel plug-in hybrid electric vehicle is built using *Matlab Simulink* and its toolbox *QSS*. A gearbox controller that selects the best gear each timestep is also included in order to control the automatic gearbox that connects the ICE with the front shaft. Furthermore, two different energy management strategies are implemented and compared mainly in terms of fuel consumption and battery SOC profile for various driving cycle conditions and different battery discharging modes. A rule-based strategy is compared with the Equivalent Consumption Minimization Strategy (ECMS) which is based on optimization algorithms.

The results show that the ECMS strategy reduces the fuel consumption in the range of 8-20 % depending on the driving cycle and battery discharge strategy compared to the rule-based strategy. Moreover, a PHEV model without generator is also modeled in order to analyze the influence of the generator on fuel consumption. The fuel consumption significantly increases due to the generator removal in all studied cases and the battery SOC profiles show higher variations from its reference value. Finally, some future work suggestion are pointed out in order to guide further researches in this topic.

Keywords: Series-Parallel Plug-in Hybrid Electric Vehicle, Energy Management, Rule-based Strategy, Optimization-based Strategy, ECMS, Battery Depleting, Battery Sustaining, NEDC, Fuel Consumption Minimization.

# Acknowledgements

First of all, I would like to thank my examiner at Chalmers, Professor Torbjörn Thiringer, and my thesis supervisor, Evelina Wikner, for giving me the opportunity of working in this project and for their helpful advices.

Second, I would like to thank my family for their love and the enormous sacrifices they have done to give me the chance of studying abroad.

Last but not least, I would like to thank all the people that I have met during my stay in Sweden. A huge amount of awesome new friends who will be in my heart forever.

David Cid Fernández, Göteborg, May 2016

# Contents

# 1
# Introduction

Nowadays, cities are the core in terms of energy consumption related to transport. This is mainly because of economic activity concentration, high volume of population and especially the increasing mobility needs. Moreover, transport is one of the main sources of noise and pollutant emissions into the atmosphere.

The European Union has formulated ambitious objectives for 2020. One of the targets is to reduce the overall greenhouse gas emissions by at least 20% compared to 1990 levels [1]. The fact that transport is responsible for a major part of the emitted greenhouse gases [2], and the ongoing reduced usage of oil have led to an increased popularity of electric and hybrid vehicles [3]. Figure 1.1 shows the european electric and hybrid electric vehicles sales along the years.

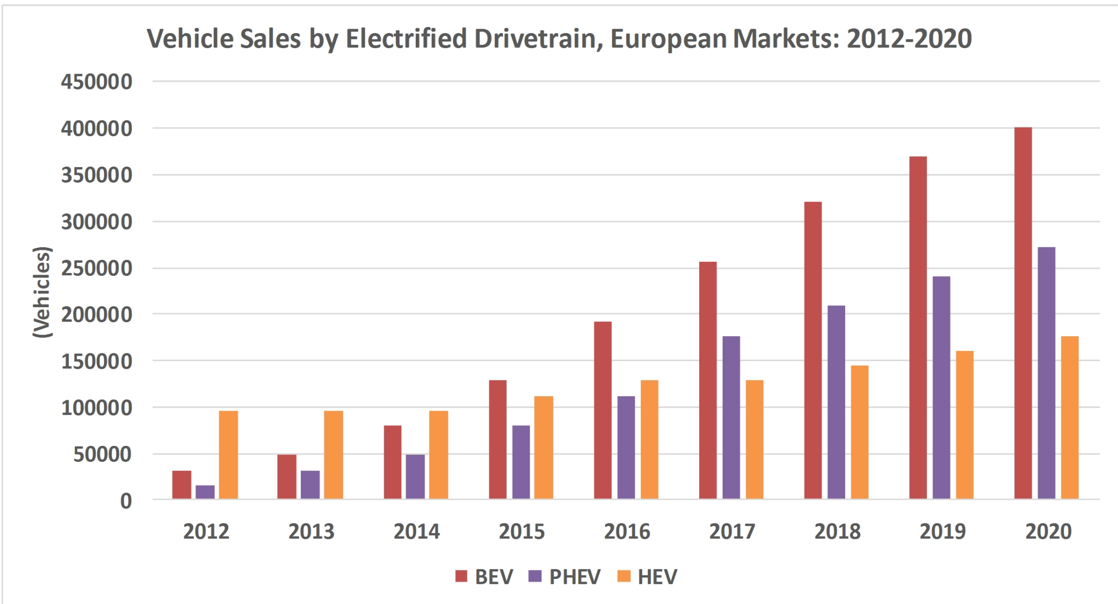


**Figure 1.1:** European electric and hybrid vehicles sales.

Electric and hybrid electric vehicles is not something new. Back in 1890, a rocket-shaped electric vehicle called *La Jamais Contente* first exceeded 100 $km/h$ and established a speed record. Around same epoch, Ferdinand Porsche developed the first hybrid vehicle, the *Lohner-Porsche Mixte Hybrid*. Since then, more electric and hybrid vehicles have been developed in the automotive industry, being more competitive everyday.

## 1.1 Problem background

Since hybrid electric vehicles combine an internal combustion engine with one or more electric machines, its control becomes really important but challenging at the same time. The control unit of hybrid vehicles is the core of the powertrain and its main function is to manage the available energy in an efficient way. The energy management algorithms split the instantaneous vehicle requested power between the different machines, in such a way that components are operated at high efficiency operating points, an adequate reserve of energy in the battery is available, the vehicle performance is not sacrificed and emissions and fuel consumption is reduced.

Rule-based control strategies, based on engineer intuition, are often used. The control law is simple and it is implementable in a contoller unit. However, other type of control strategies, known as Optimization-based strategies, could lead to better fuel consumptions. Moreover, with some kind of future prediction (using GPS, maps, radar, etc) the energy management could be combined with load prediction. Therefore, almost the optimal control signals could be find, leading to the best fuel consumption minimization. However, in order to make these strategies become a part of modern hybrid vehicles, more studies related to this kind of energy management strategies are needed.

## 1.2 Purpose of the work

The purpose of the thesis is to build a model of a series-parallel plug-in hybrid electric vehicle using *Matlab Simulink* and its toolbox for vehicle modeling *QSS* [4]. As it is explained in Chapter 2, this kind of vehicle has an internal combustion engine and two electric machines. The electric motor propels the rear wheels through a fixed gear. In the front shaft, the combustion engine is combined with an automatic gearbox and an integrated starter generator, which also recharges the battery or helps the ICE during high accelerations. Moreover a goal is to build the model of a gearbox controller that selects the best gear ratio in each timestep. Furthermore, an objective is to derive control strategies for energy-efficient operation of the vehicle and to measure energy consumption in both electric and hybrid-electric propulsion for different drive cycles. Two different energy management strategies are modeled and compared: a rule-based strategy and an optimization-based strategy, know as Equivalent Consumption Minimization Strategy (ECMS).

## 1.3 Outline

This thesis report is divided into eight chapters. The present chapter gives a brief introduction and the main objectives of this thesis. Following, in Chapter 2, the different powertrain configurations for hybrid vehicles and their possible energy management control strategies are explained. Chapter 3 provides the model description, where the mathematical equations of each component are set. Their parameters are stated in Chapter 4. After setting up the model, the different implemented energy management strategies are explained in Chapter 5. The comparison between the control strategies and a sensitivity analysis are included in Chapters 6 and 7 respectively. The report ends with Chapter 8, where the main conclusions of the work are summarized.

# 2

# Background Theory

## 2.1 Hybrid Electric Vehicle Configurations

Hybrid vehicles are those where two or more energy sources are combined to propel the vehicle. The best known technology are hybrid electric vehicles (HEV) which couple an internal combustion engine (ICE) with one or more electric machines. A HEV can be classified mainly into three different topologies [6]: series-hybrid, parallel-hybrid and series-parallel hybrid. Plug-in hybrid electric vehicles are another topology which allows the battery to be charged using electricity from the grid. These vehicles have demonstrated good fuel consumption and performance [7] so they are becoming very popular and most automakers are focusing on them.

### 2.1.1 Series HEV

In series hybrid vehicles the responsible for vehicle propulsion is only the electric motor (EM). The difference with a pure electric vehicle is that the energy does not come exclusively from a battery recharged by the grid, but also the battery is recharged partially or completely by an internal combustion engine. The combustion engine is coupled, either directly or through a gearbox, to an electric generator (EG) which transforms the mechanical power to electrical power to charge the battery or to feed the EM.

In this configuration, the electric motor drives the vehicle alone so it must be designed for the maximum power requirements. However, the ICE can be downsized and as it is mechanically decoupled from the wheels it can be set to operate at points of maximum efficiency.
In Fig. 2.1 the scheme of this type of configuration is outlined.

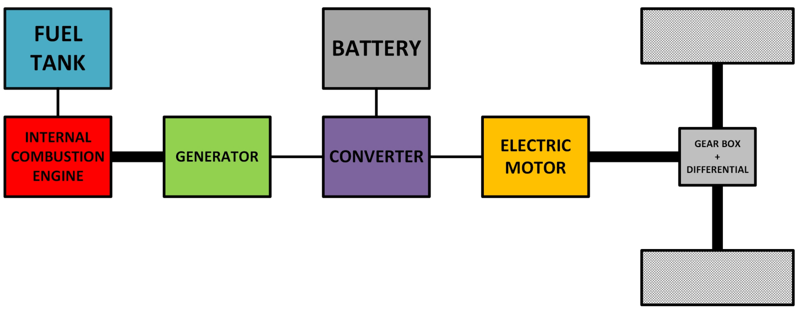


**Figure 2.1:** Series hybrid vehicle configuration.

### 2.1.2 Parallel HEV

A parallel hybrid vehicle is characterized by an internal combustion engine mechanically connected to the wheels and an electric motor also connected to the wheels. Therefore, both the ICE and the EM supply the traction power to propel the vehicle. As the total traction power is a combination of both motors, the size of the machines can be set for a part of the maximum required power.

When the vehicle is propelled only with the EM, the engine can be disconnected, whereas on the other hand, when the ICE is driving the vehicle, the EM is connected and it can be utilized as a generator to charge the battery by regenerative braking or by power provided by the ICE.

Regarding the position of the EM with respect to the conventional drive train, the parallel hybrid vehicles can be classified into 4 topologies [5]:

1. *Micro hybrids*, where the EM is belt-driven or crankshaft mounted on the front of the ICE so its speed is always linked to that of the engine.
2. *Pre-transmission parallel hybrids*, where the EM is mounted between the ICE and the gearbox. This configuration is also called *single-shaft*.
3. *Post-transmission or double-shaft parallel hybrids*, where the EM is mounted downstream of the gearbox.
4. *Through-the-road or doubledrive parallel hybrids*, where the ICE and the EM are mounted on two different shafts.

In Fig. 2.2 the scheme of a parallel hybrid is outlined.

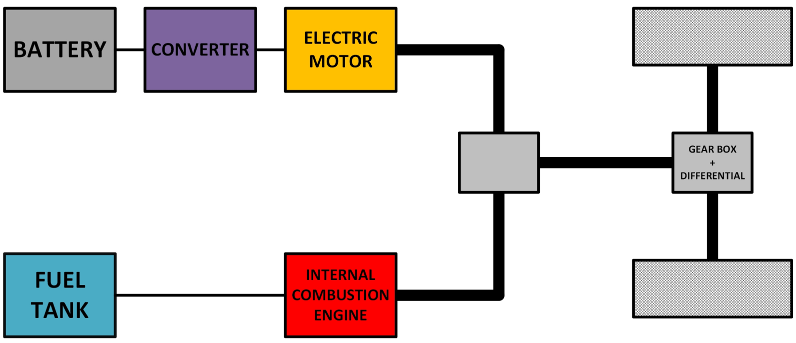


**Figure 2.2:** Parallel hybrid vehicle configuration.

### 2.1.3 Series-Parallel or Combined HEV

A combined HEV is a parallel hybrid but it incorporates some of the advantages of the series hybrids. The vehicle can operate in pure electric mode, in combustion engine mode or in combined mode. The big difference with the parallel-hybrid is when operating in the combined mode: the combustion engine drives a generator (as it happens in the series hybrids) that powers the electric motor, charges the batteries or it is used for the stop-and-start operation. Furthermore, it can operate in serial mode using the combustion engine only to power the generator. They incorporate a complex power split device. An example of this configuration is Toyota Prius. In Fig. 2.3 the scheme of a combined hybrid is outlined.

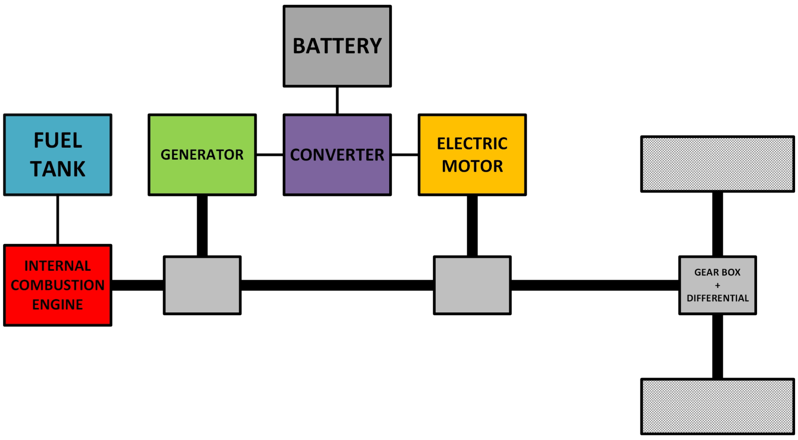


**Figure 2.3:** Series-Parallel hybrid vehicle configuration.

## 2.2 Classification of Energy Management Control Strategies for HEVs

As it was said before, a HEV is equipped with two or more energy sources and machines. The role of the energy management control strategy is not only the co-ordination of the energy sources but also the power flow control for the mechanical and electrical path. It consists of an algorithm implemented in the control unit of the vehicle, which based on several inputs (e.g. vehicle speed, acceleration, SOC of the battery, traffic information...) and on the chosen regulating law, makes decisions like turning on or off certain components or changing their operation points.

Since the configuration of each HEV topology is different, diverse energy management control strategies are needed. However, all of them aim to achieve similar main goals [8]:

- Maximize fuel economy
- Minimize emissions
- Minimize system cost
- Good driving performance

There are mainly two general trends dealing with the energy management: rule-based control strategies and optimization-based control strategies. Based on the review article [9], the following sections summarize the concepts of various types of control strategies for hybrid electric vehicles. The mathematical formulation of each strategy can also be found in [9]. Figure 2.4 shows a classification of the HEV control strategies.

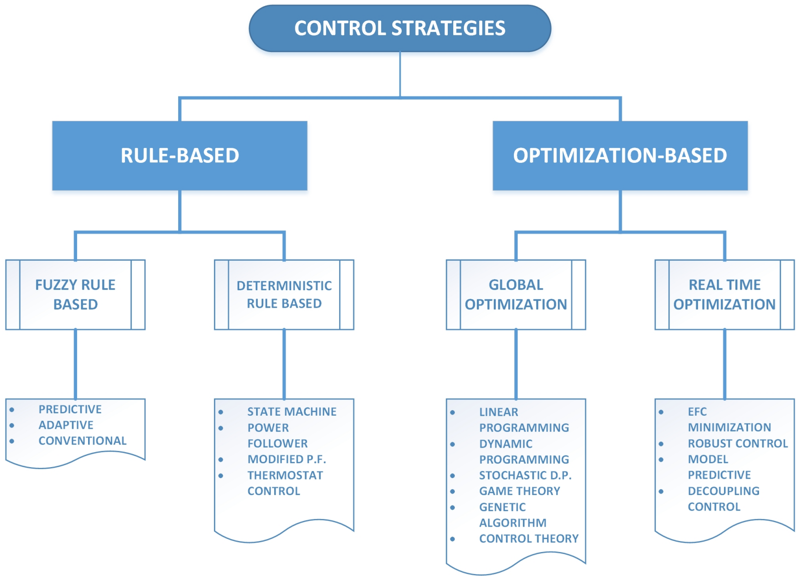


**Figure 2.4:** Classification of the hybrid power train control strategies.

### 2.2.1 Rule-Based Control Strategies

The rules of this sort of strategies are based on heuristics, experience, intuition, etc. Their main idea is to shift the actual ICE operating point to another point with the highest possible efficiency at a particular engine speed. The difference between the required power to propel the vehicle and the power provided by the ICE will be compensated by the EM or used to charge the battery, depending on the SOC. Control strategies based on rules can be classified into deterministic and fuzzy rule based approaches.

#### 2.2.1.1 Deterministic Rule-Based Strategies

Lookup tables are used in order to split the requested power between the different power converters. The main deterministic rule-based control strategies include the following:

- Thermostat (on/off) Control Strategy
- Power Follower (Baseline) Control Strategy
- Modified Power Follower (Base Line) Strategy
- State Machine-Based Strategy

#### 2.2.1.2 Fuzzy Rule-Based Methods

Fuzzy logic controllers are an extension of the conventional rule-based ones. These strategies consider the dynamic nature of the system when performing the optimization and they could lead to a real-time and suboptimal power split. The foremost fuzzy logic strategies are the following:

– Conventional Fuzzy Strategy
– Fuzzy Adaptive Strategy
– Fuzzy Predictive Strategy

### 2.2.2 Optimization-Based Control Strategies

The key factor of these control strategies is that the optimal control settings (e.g. gear ratios, power split...) are achieved by minimization of a cost function that usually represents the fuel consumption or emissions. A global optimal solution can be found if the driving cycle is known in advance. Therefore, these approaches cannot be used for real-time energy management. However, by defining an instantaneous cost function (e.g. equivalent fuel consumption) a real-time local optimum solution could be found.

#### 2.2.2.1 Global Optimization

There are numerous algorithms that can perform a global optimum operating point but their computational complexity limits their practical application. However, they are good tools to analyze and compare other control strategies. The main global optimization algorithms are:

– Simulated Annealing
– Game Theory
– Linear Programming
– Optimal Control Theory
– Dynamic and Stochastic Programming
– Genetic Algorithms

#### 2.2.2.2 Real-Time Optimization

As stated before, global optimization techniques cannot be implemented for real-time control strategies because they lead to casual solutions, meaning that they depend on past and future events. Real-time optimization strategies implement a cost function taking into account not only fuel consumption but also variations of the state of charge of the battery to guarantee the self-sustainability. The instantaneous optimization of this cost function bring suboptimal solutions but they can be used in real-time control. The most known real-time optimization techniques are the following:

– Real-Time Control Based on Equivalent Fuel Consumption
– Decoupling Control
– Robust Control Approach
– Optimal Predictive Control

# 3

# Model Description

## 3.1 Series-Parallel Plug-in Hybrid Electric Vehicle

The vehicle chosen for this thesis is a luxury high-performance series-parallel plug-in hybrid electric mid size Station Wagon, similar to the one sketched in Fig. 2.3. The electric motor propels the rear wheels through a fixed gear, while most of the job rests on the gasoline ICE in the front shaft. The combustion engine is combined with an automatic gearbox and an integrated starter generator, which also recharges the battery or helps the ICE during high accelerations. Both electric machines could recover energy through regenerative braking. The vehicle is also equipped with a battery and a control unit which is responsible for the energy management control.

These components within the powertrain are modeled separately and are connected between them. The modeling approach used is called quasistatic modeling or backward modeling. It is a kind of simulation in which one knows what the system has made, the vehicle in this case, and from that point the operating conditions are calculated. Therefore, as shown in Fig. 3.1 based on a chosen drive cycle, the resistance forces which act on the vehicle are calculated. After that, the required power to drive along the drive cycle is also calculated backwards within the powertrain. This power results in a fuel consumption for the ICE or in a variation of the state of charge of the battery.

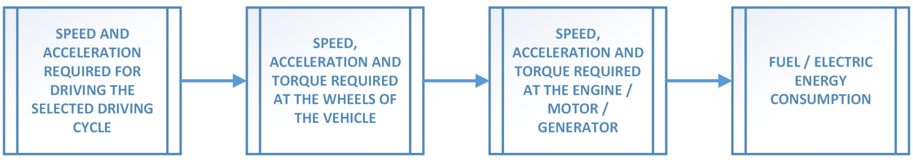


**Figure 3.1:** Quasistatic or backward modeling.

The equations described in [5] for each component and the QSS-toolbox for Matlab Simulink [4] have been used to build this model. However, some basic models have been modified when needed.

## 3.2 Longitudinal Vehicle Model

The basic equation that describes the longitudinal dynamics of a vehicle is Newton's second law of motion and has the following form

$$m_v \frac{d}{dt} v(t) = F_t(t) - (F_a(t) + F_r(t) + F_g(t)) \tag{3.1}$$

where $F_a(t)$ refers to aerodynamic friction, $F_r(t)$ the rolling friction, $F_g(t)$ the gravitational force, $F_t(t)$ the traction force produced by the powertrain, $m_v$ the mass of the vehicle and $v(t)$ is the vehicle velocity. Fig. 3.2 shows a representation of this equation.

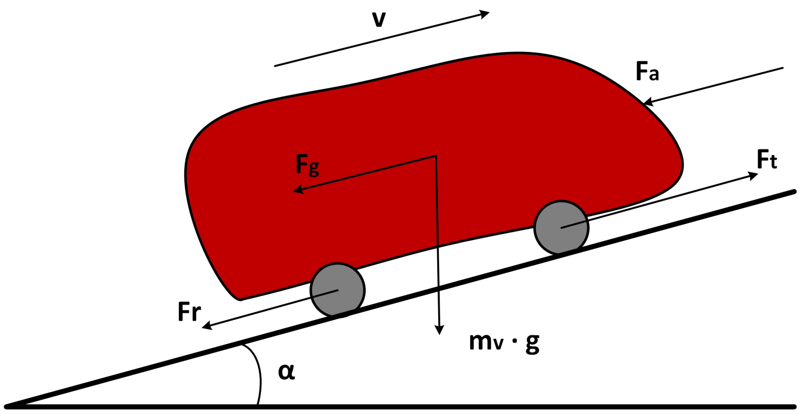


**Figure 3.2:** Forces acting on a vehicle.

### Aerodynamic Friction Force

The aerodynamic resistance $F_a$ is modeled as if the vehicle was a prismatic body with a frontal area $A_f$ and an aerodynamic drag coefficient $cd(v, ...)$ which is taken constant in this model. Its equation is

$$F_a(v) = \frac{1}{2}\, \rho_a\, A_f\, cd(v, ...)\, v^2 \tag{3.2}$$

where $v$ is the vehicle speed and $\rho_a$ is the air density.

### Rolling Friction Force

The rolling resistance is modeled as

$$F_r(v, p, ...) = c_r(v, p, ...)\, m_v\, g\, \cos(\alpha), \qquad v > 0, \tag{3.3}$$

where $m_v$ is the vehicle mass, $g$ the gravity acceleration, $\alpha$ the inclination angle of the road and $c_r$ the rolling friction coefficient. This coefficient depends on several variables (e.g. vehicle speed, tire pressure...) but in this model it is taken constant. Moreover, $\alpha$ is constant and 0 for all driving cycles used in this model.

### Gravitational Force

The gravitational force is modeled as

$$F_g(\alpha) = m_v\ g\ \sin(\alpha), \tag{3.4}$$

which can be approximated for small inclinations $\alpha$ as

$$F_g(\alpha) = m_v\ g\ \alpha. \tag{3.5}$$

In this analysis, $F_g$ remains equal to 0 due to the horizontal road inclination in the used driving cycles.

### Traction Force

The required or traction force $F_t$ to propel de vehicle with a certain acceleration is given by (3.1). The required torque in the wheels $T_w$ associated to the traction force $F_t$ is given by

$$T_w = F_t\ r_w, \tag{3.6}$$

where $r_w$ is the wheel radius. Thus, the required power to propel the vehicle at a certain speed $v$ is calculated as

$$P_w = T_w\ w_w = T_w\ \frac{v}{r_w}, \tag{3.7}$$

where $w_w$ is the angular wheel speed.

Depending on the value of $F_t$ the vehicle can operate in three different modes:

- $F_t > 0$ , traction mode: the powertrain provides a propulsion force to the vehicle;
- $F_t < 0$ , braking mode: the brakes act dissipating kinetic energy of the vehicle or this energy is recovered by electric machines and is stored in the battery (regenerative braking);
- $F_t = 0$ , coasting mode: the powertrain is disengaged and the vehicle loses energy due to the resistance losses.

## 3.3 Internal Combustion Engine Model

This block in the model simulates the behavior of an internal combustion engine in terms of fuel consumption.

As the formulation used is the quasistatic approach, the inputs to this block are the angular velocity $w_e$ and angular acceleration $dw_e$ at which the engine rotates and the torque $T_e$ that it produces. The output is the equivalent power $P_c$ to the fuel that the engine is consuming. Taking into account the torque that the engine supplies and its rotational speed, the instantaneous fuel consumption is calculated from the consumption map. The efficiency of the engine is calculated as

$$\eta_e = \frac{w_e\, T_e}{P_c} \tag{3.8}$$

and it is often plotted in the form of an engine map.

$P_c$ is related to the fuel mass flow by

$$\dot{m}_f = P_c/H_l, \tag{3.9}$$

where $H_l$ is the fuel's lower heating value.

There are two normalized variables that describe the engine operating point when it runs in steady-state conditions. The mean piston speed

$$c_m = \frac{w_e\, S}{\pi} \tag{3.10}$$

and the mean effective pressure

$$p_{me} = \frac{N\, \pi\, T_e}{V_d} \tag{3.11}$$

where $V_d$ is the engine's displacement, $S$ its stroke and $N$ a parameter that depends on the engine type: for a four-stroke engine $N = 4$ and for a two-stroke engine $N = 2$.

For a fixed mean effective pressure and a mean piston speed, the mechanical power $P_e$ produced by the engine is calculated by

$$P_e = z\, \frac{\pi}{16}\, B^2\, p_{me}\, c_m \tag{3.12}$$

where $z$ is the number of cylinders and $B$ the cylinder bore.

## 3.4 Electric Motor / Generator Model

Following the quasistatic approach, the inputs for the electric motor model are the torque $T_{gear}$, the angular speed $w_{gear}$ and the angular acceleration $dw_{gear}$ required at the gearbox that precedes the motor. The output is the electric power required at the DC link $P_{EM}$, which is positive when the machine operates as a motor and negative when it operates as a generator.

The total torque that the motor has to provide is calculated as

$$T_{EM} = T_{gear} + \theta_{EM}\, dw_{gear} \tag{3.13}$$

where $\theta_{EM}$ is the inertia of the motor. The motor speed remains the same as the input, thus

$$w_{EM} = w_{gear}. \tag{3.14}$$

The relation between the electric power $P_{EM}$ and the mechanical power $T_{EM}\, w_{EM}$ is calculated using an efficiency map of the machine. This map gives the efficiency of the motor $\eta_m$ as a function of $T_{EM}$ and $w_{EM}$. Therefore, the required electric power is calculated as

$$P_{EM} = \frac{T_{EM}\ w_{EM}}{\eta_m(w_{EM}, T_{EM})} \qquad T_{EM} \geq 0, \tag{3.15}$$

$$P_{EM} = T_{EM}\ w_{EM}\ \eta_m(w_{EM}, T_{EM}) \qquad T_{EM} < 0. \tag{3.16}$$

In order to facilitate the calculations, when entering the efficiency map data, the stored data is $1/\eta_m$ in the region where torque is positive.

The model of a generator is quite similar to the motor's model. There are only two differences: the efficiency map only includes the data of the generator mode and the model does not take into account the inertia of the generator.

## 3.5 Gear-Box Model

Gear boxes are devices that transform the mechanical power provided by a power source at a certain angular speed $w_1$ and torque $T_1$ to a different angular speed $w_2$ and torque $T_2$.

There are mainly three types of gear boxes:

- Manual gear boxes: they have a finite number of fixed gear ratios and are manually operated by the driver.
- Automatic transmissions: they have a fixed number of gear ratios and an automated gear shift mechanism.
- Continuously variable transmissions (CVTs): they can provide any desired gear ratio within the limits of this device.

Following the quasistatic approach, the inputs of this block are angular speed $w_{wheel}$, angular acceleration $dw_{wheel}$ and torque $T_{wheel}$ in the wheels. The outputs are angular speed $w_{trans}$, angular acceleration $dw_{trans}$ and torque in the engine $T_{trans}$. The outputs are calculated taking into account the gear ratio $\gamma$, the efficiency $\eta_{gb}$ and the losses in the transmission elements between the wheels and the engine $P_0$.

The engine angular speed is calculated by

$$w_{trans} = w_{wheel}\ \gamma \tag{3.17}$$

and the engine angular acceleration by

$$dw_{trans} = dw_{wheel}\ \gamma. \tag{3.18}$$

The engine torque is calculated as follows, depending on the sign of $T_{wheel}$:

$$T_{trans} = \frac{T_{wheel} + \frac{P_0}{w_{wheel}}}{\gamma\ \eta_{gb}}, \qquad if\ T_{wheel} > 0 \tag{3.19}$$

or

$$T_{trans} = \frac{T_{wheel} + \frac{P_0}{w_{wheel}}}{\gamma}\ \eta_{gb}, \qquad if\ T_{wheel} < 0 \tag{3.20}$$

## 3.6 Energy Storage System Model

The model of the battery has been built following the procedure presented in article [10]. This article presents a battery cell model that only uses the battery State-Of-Charge (SOC) as a state variable and that can represent four different types of battery chemistries. The model's parameters have to be obtained from the manufacturer's discharge curve but the article provides them for four different cells.

The cell model is based on a simple controlled voltage source in series with a constant resistance. The open voltage source can be calculated with a non-linear equation based on the actual SOC. This equation is

$$E = E_0 - K \frac{Q}{Q - \int i_{batt} dt} + A\, e^{-B\, \int i_{batt} dt} \tag{3.21}$$

where

$E$ = no-load voltage (V)
$E_0$ = cell constant voltage (V)
$K$ = polarisation voltage (V)
$Q$ = cell capacity (Ah)
$\int i_{batt} dt$ = actual cell charge (Ah)
$A$ = exponential zone amplitude (V)
$B$ = exponential zone time constant inverse $(Ah)^{-1}$
$i_{batt}$ = cell current (A).

The cell terminal voltage is calculated as

$$V_{batt} = E - R\, i_{batt} \tag{3.22}$$

where $R$ is the internal resistance ($\Omega$).

Consequently, taking into account this cell model and the number of series and parallel cells required for a certain battery voltage and battery capacity, the model of the battery is built. Its inputs are the terminal power $P_{BT}$ and the total driven distance. The outputs are the battery terminal voltage, the battery SOC, the battery efficiency and the energy consumption per km.

## 3.7 Driving Cycles

The test driving cycles are standardized speed and elevation profiles that have been introduced in order to compare pollutant emissions and fuel economy of different vehicles on the same basis.
These driving cycles are regulated in the European Union, in the United States and in Japan and are called standard driving cycles. They are always performed assuming that the car is running on zero slope roads.

In the United States, the FTP 72, SFUDS, FTP 75, HFEDS, IM 240, LA-92, and US NYCC 06 are the most typical test cycles. Figure 3.3 shows FTP 75 test cycle.

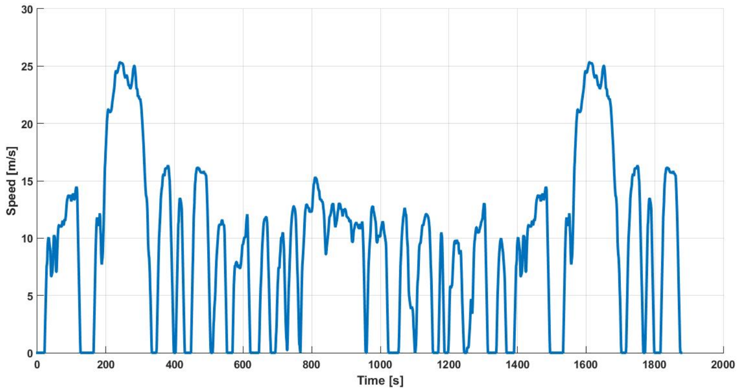


**Figure 3.3:** FTP-75 test cycle.

In Japan, the cycles that are most often used are Mode 10, Mode 15 and Mode 10-15. Figure 3.4 shows Mode 10-15 test cycle.

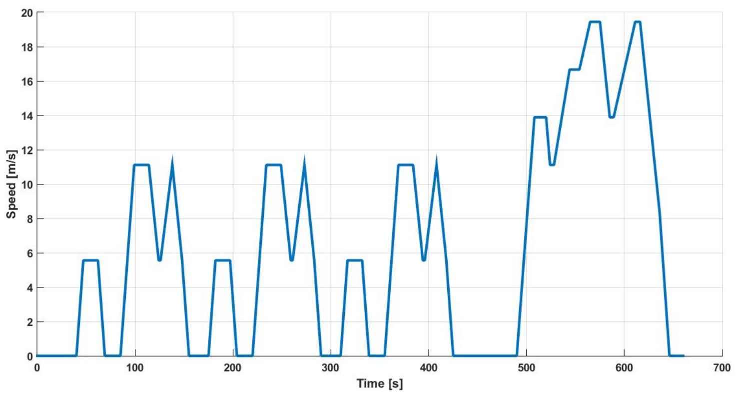


**Figure 3.4:** Mode 10-15 test cycle.

In Europe, the most used are the cycle ECE-15, the EUDC, the EUDCL and the NEDC. The last one is the official cycle to standardize pollutant emissions and vehicle autonomy in Europe. It is also known as MVEG-95 and it is a combination of 4 cycles ECE-15 (city cycle) and one EUDC cycle at the end (highway cycle). The cycle time is 1180 seconds. Figure 3.5 shows NEDC test cycle.

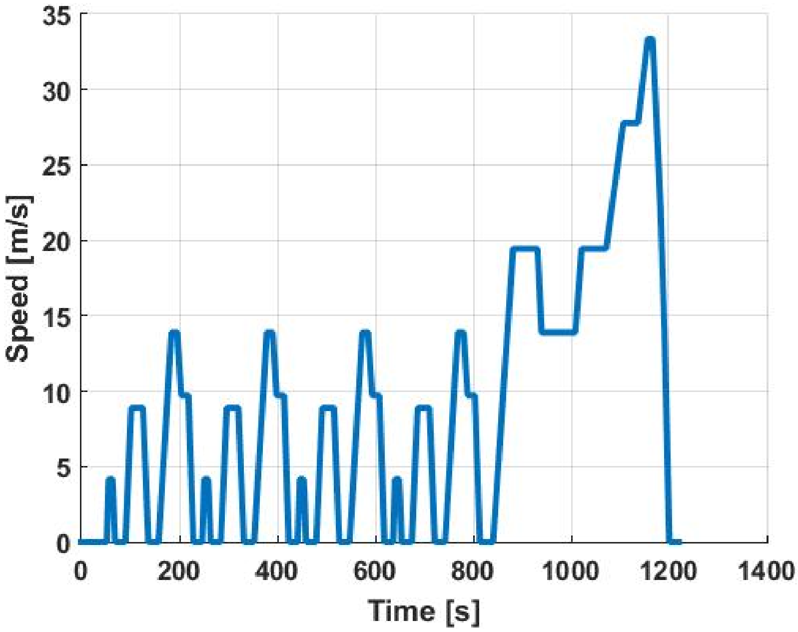


**Figure 3.5:** NEDC test cycle.

# 4

# Model set-up

As mentioned in Section 3.1, the vehicle studied in this thesis is a series-parallel hybrid electric mid size Station Wagon. It has an ICE with an integrated starter EG in the front shaft and an EM mounted in the rear shaft. In this chapter, the specifications of the powertrain are set.

## 4.1 Vehicle Parameters

The vehicle parameters are summarized in Table 4.1.

**Table 4.1:** Vehicle Parameters

| **Parameter** | **Value** |
|---|---|
| Curb weight | 1600 kg |
| Rotating mass | 5 % |
| Cross section | 2 $m^2$ |
| Wheel diameter | 0.6 m |
| Drag coefficient | 0.29 |
| Rolling friction coefficient | 0.01 |

## 4.2 Internal Combustion Engine Specifications

The ICE parameters are collected in Table 4.2.

**Table 4.2:** Internal Combustion Engine Specifications

| **Parameter** | **Value** |
|---|---|
| Fuel | Gasoline |
| Fuel low heating value | 42.7 MJ/kg |
| Fuel density | 0.745 kg/l |
| Maximum power | 160 kW |
| Maximum torque | 331 Nm |
| Maximum speed | 628 rad/s |

The ICE consumption map is shown in Figure 4.1.

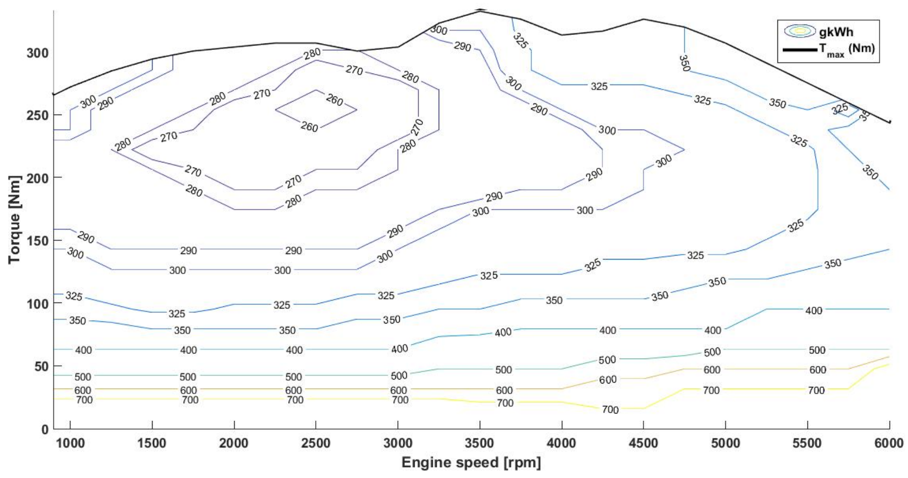


**Figure 4.1:** ICE consumption map.

## 4.3 Integrated Starter Generator Specifications

Table 4.3 shows the integrated starter electric generator parameters.

**Table 4.3:** Itegrated Starter Electric Generator Specifications

| **Parameter** | **Value** |
|---|---|
| Maximum power | 34 kW |
| Maximum torque | 63 Nm |
| Nominal speed | 487 rad/s |
| Maximum speed | 1950 rad/s |

The EG efficiency map is shown in Figure 4.2.

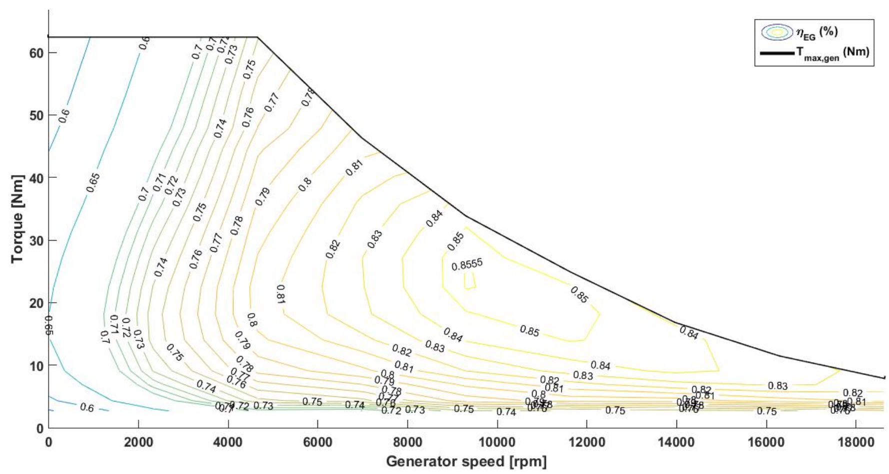


**Figure 4.2:** EG efficiency map.

## 4.4 Electric Motor Specifications

Table 4.4 summarizes the electric motor parameters.

**Table 4.4:** Electric Motor Specifications

| Parameter | Value |
|---|---|
| Maximum power | 52.2 kW |
| Maximum torque | 312.31 Nm |
| Nominal speed | 150 rad/s |
| Maximum speed | 600 rad/s |

The EM efficiency map is shown in Figure 4.3.

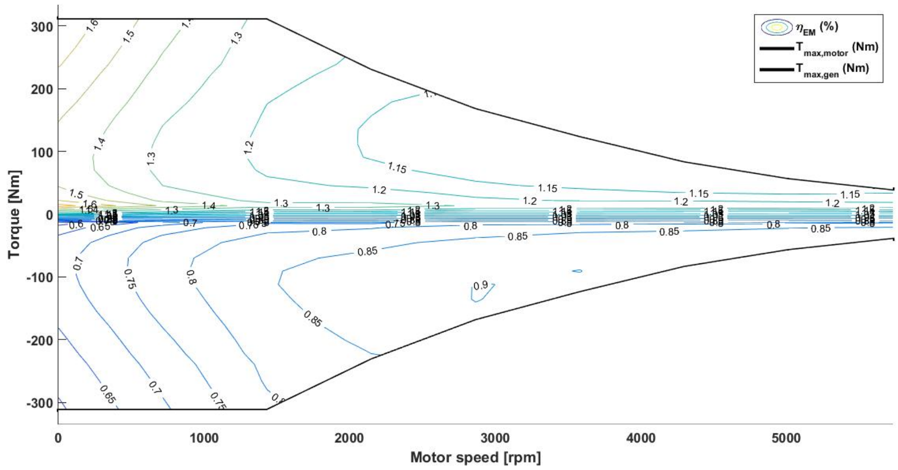


**Figure 4.3:** EM efficiency map.

Note that, in order to facilitate the calculations, the stored data is $1/\eta_m$ in the region where torque is positive.

## 4.5 Transmission Systems Parameters

The parameters of the different transmission systems modeled in this thesis are collected in Tables 4.5, 4.6 and 4.7.

**Table 4.5:** EM Transmission Parameters

| Parameter | Value |
|---|---|
| Type | Fixed gear |
| Gear ratio | 5 |
| Efficiency | 0.98 |
| Idling losses | 0 W |

**Table 4.6:** ICE Transmission Parameters

| Parameter | Value |
|---|---|
| Type | Automatic |
| Number of gears | 6 |
| $1^{st}$ gear ratio | 4.148 |
| $2^{nd}$ gear ratio | 2.370 |
| $3^{rd}$ gear ratio | 1.556 |
| $4^{th}$ gear ratio | 1.155 |
| $5^{th}$ gear ratio | 0.850 |
| $6^{th}$ gear ratio | 0.686 |
| Differential gear | 3.2 |
| Efficiency | 0.98 |
| Idling losses | 0 W |

**Table 4.7:** EG Transmission Parameters

| Parameter | Value |
|---|---|
| Type | Fixed gear |
| Gear ratio | 2.2 |
| Efficiency | 0.98 |
| Idling losses | 0 W |

## 4.6 Energy Storage System Parameters

The specifications of the energy storage system used in this thesis are shown in Table 4.8. For a better understanding of them, see Section 3.6.

**Table 4.8:** Battery parameters

| Parameter | Value |
|---|---|
| Cell type | Lithium-Ion |
| Cell constant voltage | 3.7348 V |
| Polarisation voltage | 0.00876 V |
| Cell internal resistance | 0.09 Ω |
| Cell capacity | 1 Ah |
| Exponential zone amplitude | 0.468 V |
| Exponential zone time constant inverse | 3.5294 $(Ah)^{-1}$ |
| Nº of cells connected in series | 100 |
| Nº of cells connected in parallel | 33 |
| Total battery capacity | 12 kWh |

# 5

# Implemented Energy Efficient Control Strategies

In this chapter, the different methods implemented in order to get a low fuel consumption of the studied vehicle are explained.

## 5.1 Energy Efficient Gearbox Controller

In the modeled vehicle, the ICE is connected in the front shaft through an automatic gearbox, whose parameters are specified in Table 4.6. Therefore, an algorithm that selects the best gear ratio in each timestep is needed.

Based on the required torque in the front shaft $T_{fgb}$, angular speed $w_{fgb}$ and acceleration $dw_{fgb}$, the torque $T_{ice}$, angular speed $w_{ice}$ and acceleration $dw_{ice}$ that the ICE would have for each different gear ratio are calculated. Later, these ICE operating points ($T_{ice}$,$w_{ice}$) for each gear ratio are checked in order to fulfill the ICE limitations. For those that meet the requirements (below maximum ICE torque and speed), the corresponding fuel consumption is computed. Finally, the gear ratio that provides the lowest fuel consumption is chosen. Figure 5.1 shows an example of which gear would be selected according to the algorithm described above.

However, this gearbox controller has an important difference compare with a real automatic gearbox. In the modeled controller, the gear is shifted every timestep (1 second), trying to find always the most efficiency operating point. In a real world gearbox this situation is unfeasible. This issue could be solved by adding a minimum time delay between each gear shift. However, as the main purpose of this thesis is to compare the following two Energy Management Strategies and in order to not influence the fuel consumption results, the gearbox controller has been kept as explained in the previous paragraph.

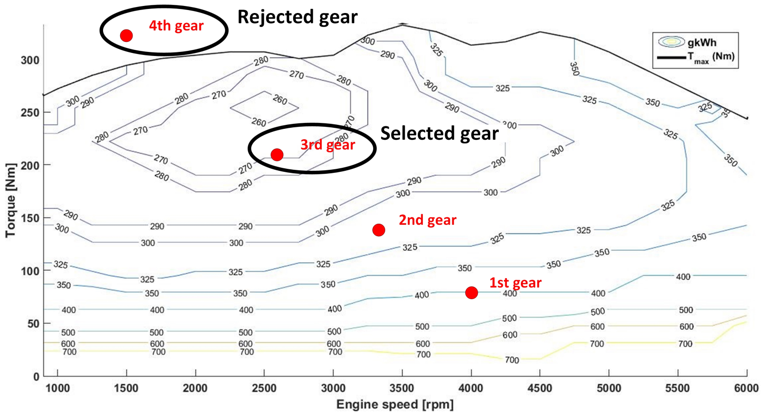


**Figure 5.1:** Example of gearbox controller choosing the right gear ratio.

## 5.2 Energy Management Strategies

As mentioned in Section 2.2, the role of the energy management control strategy is to determine the power split between the ICE, EM and EG, base on a requested torque. The objective is mainly to maximize the fuel economy while keeping the constraints due to driveability requirements and the characteristics of the components. There are mainly two groups of energy management control strategies [9]: rule-based and optimization-based strategies. However, among them there are hundreds of different algorithms. Two of them have been chosen to be implemented in this thesis and are explained below.

### 5.2.1 Rule-Based Strategy

A rule-based control strategy is a set of rules that determines when to use the ICE, the EM, the EG or a combination of them. The main idea is to operate the ICE at the highest possible efficiency points. Most of the HEV and PHEV nowadays use this kind of energy management strategies. One of them, described in [11], is the baseline of the rule-based strategy implemented in this thesis. Its operation is explained below.

Taking into account the battery SOC and the required torque to propel the vehicle, the control unit decides if the vehicle is only propelled by ICE, EM, or by a combination of both machines. Moreover, as the vehicle is equipped with an EG, this machine can be used to charge the battery.

1. If the required torque is negative, i.e. during braking, the EM acts as a generator, charging the battery through regenerative braking.

2. When the battery SOC is between the minimum and maximum values (25% and 80%), the ICE does not work below a certain speed (120 rad/s) and a certain torque, defined as a fraction of the maximum torque (20% of max. ICE torque), unless the vehicle is in operational mode 4. These minimum

and maximum values of battery SOC have been chosen in order to reduce premature battery aging [12]. The minimum ICE toque has been chosen in order to avoid the lowest efficiency working area of the ICE.

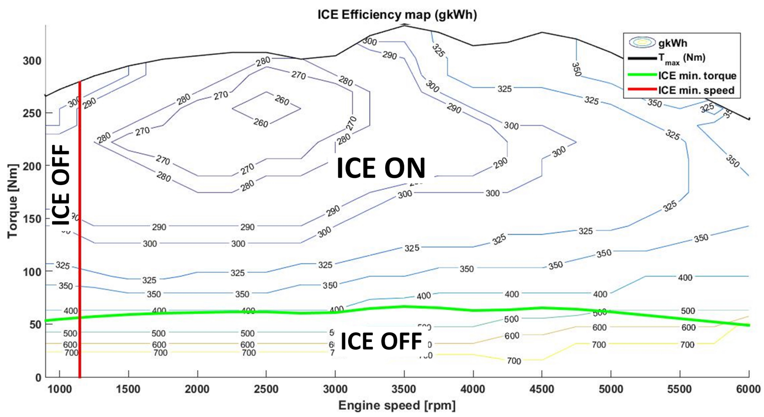


**Figure 5.2:** ICE working areas for Rule-Base Control Strategy

3. When the battery SOC is below the lower limit, the ICE works according to the following two different situations:

   (a) If the engine was previously ON, its torque is increased 30% in order to supply some extra torque to the EG and charge the battery. The ICE is always limited to its maximum torque.

   (b) If the engine was previously OFF, it works exactly at the minimum torque set in 2 (20% of max. ICE torque). The difference between this torque and the required torque to propel the vehicle is sent to the EG to charge the battery.

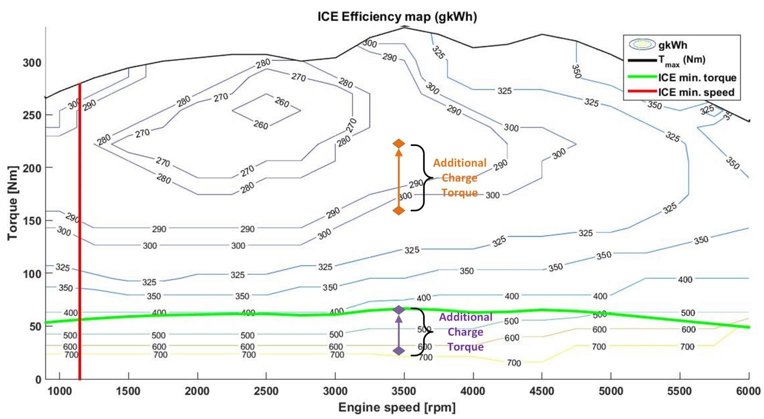


**Figure 5.3:** ICE additional charge torque for Rule-Base Control Strategy

4. If the EM is propelling the vehicle and the required power is higher than what the EM can provide, the ICE is turned ON and it will help to boost the vehicle,

even if this situation conflicts with situation 2.

5. Once the minimum battery SOC is reached, the battery SOC is kept between a narrow window in order to achieve a battery sustaining mode.

### 5.2.2 Optimization-Based Strategy

As stated in Section 2.2.2, an optimization-based strategy consists of trying to minimize a cost function that normally represents the fuel consumption or emissions of the vehicle. Based on specific inputs (requested torque, battery SOC...), the control unit will decide the optimal power split ratio that minimize the cost function while satisfying the constraints. In order to understand the power split ratio concept and the formulation behind optimal control strategies, a simplified powertrain model is needed. It is explained in the following section.

#### 5.2.2.1 Basic Powertrain Equations

According the model description in Chapter 3, a simplified powertrain model, where only torques, speeds, gear ratios and efficiencies are taken into account is shown in Figure 5.4. It is convenient to follow this figure in order to understand the following equations.

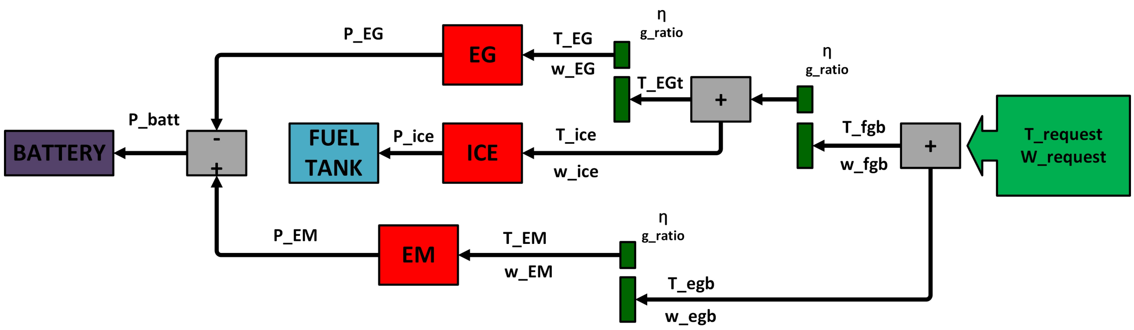


**Figure 5.4:** Simplified powertrain model

First of all, the power split ratios should be defined. The first ratio, $v$, will set how much torque is applied in the rear shaft (electric motor) regarding the requested torque. It is defined as

$$v = \frac{T_{egb}}{T_{req}} \qquad \in [0, 1] \tag{5.1}$$

where $T_{egb}$ is the torque at the rear gearbox and $T_{req}$ is the requested torque. Note that the difference between this torque and the requested torque plus the torque needed by the EG will be applied to the front shaft.

The second power split ratio, $w$, determines how much torque should by applied to the generator regarding the torque in the front shaft. Note that this generator torque has to be produced by the ICE. It is defined as

$$w = \frac{T_{EGt}}{T_{fgb}} \qquad \in [0, 1] \tag{5.2}$$

where $T_{EGt}$ is the torque applied at the EG transmission and $T_{fgb}$ represents the torque applied i the front shaft. Note that due to the selected possible values of $w$, the generator will be used to charge the battery and never to boost the vehicle.

According to the previous definitions, (5.3), (5.4) and (5.5) define the torque splits:

$$T_{egb} = T_{req}\, v \tag{5.3}$$

$$T_{fgb} = T_{req}\, (1 - v)\, (1 + w) \tag{5.4}$$

$$T_{EGt} = T_{req}\, (1 - v)\, w \tag{5.5}$$

The speed of the ICE is determined as

$$w_{ice} = w_{req}\, g_{ratio} \tag{5.6}$$

where $w_{req}$ is the required speed at the wheels of the vehicle and $g_{ratio}$ is the corresponding gear ratio of the front shaft transmission, which is given by the gearbox controller.
The ICE angular speed is calculated as

$$dw_{ice} = dw_{req}\, g_{ratio} \tag{5.7}$$

where $dw_{req}$ is the required angular acceleration at the vehicle wheels.
The ICE torque is given by

$$T_{ice} = \frac{T_{fgb}}{g_{ratio} \cdot \eta} \tag{5.8}$$

where $\eta$ represents the gearbox efficiency.

The torque that will be applied to the EM, $T_{EM}$, is determined by (5.9) and (5.10). Its angular speed $w_{EM}$ and acceleration $dw_{EM}$ by (5.11) and (5.12) respectively, where $g_{ratio}$ is the fixed gear ratio of the rear shaft transmission and $\eta$ its efficiency. Note that, due to *QSS Toolbox* references, a positive torque $T_{EM}$ will produce a positive power that will discharge the battery.

$$T_{EM} = \frac{T_{egb}}{g_{ratio} \cdot \eta} \qquad if \quad T > 0 \tag{5.9}$$

$$T_{EM} = \frac{T_{egb}}{g_{ratio}} \eta \qquad if \quad T < 0 \tag{5.10}$$

$$w_{EM} = w_{egb}\, g_{ratio} \tag{5.11}$$

$$dw_{EM} = dw_{egb}\, g_{ratio} \tag{5.12}$$

Note that $w_{egb} = w_{fgb} = w_{req}$ and $dw_{egb} = dw_{fgb} = dw_{req}$.

Regarding the electric generator, its torque is calculated as

$$T_{EG} = \frac{T_{EGt}}{g_{ratio} \cdot \eta} \tag{5.13}$$

being $g_{ratio}$ and $\eta$ the corresponding gear ratio and efficiency of the EG transmission system. Note that, due to *QSS Toolbox* references, a positive torque $T_{EG}$ will produce a positive power that will charge the battery. The EG angular speed $w_{EG}$ and acceleration $dw_{EG}$ are given by (5.14) and (5.15)

$$w_{EG} = w_{ice}\; g_{ratio} \tag{5.14}$$

$$dw_{EG} = dw_{ice}\; g_{ratio}. \tag{5.15}$$

Once the torques and speeds of each machine are determined, their power flows can be stated. The EM electrical power $P_{EM}$ can be denoted as

$$P_{EM} = (T_{EM} + dw_{EM}\; \theta)\; w_{EM}\; \eta(T_{EM}, w_{EM}) + P_{aux} \tag{5.16}$$

where $\theta$ is the motor inertia, $\eta(T_{EM}, w_{EM})$ its efficiency given by the efficiency map shown in Figure 4.3 and $P_{aux}$ auxiliary power for services like air conditioner, but it has been set to zero in this thesis.

Regarding the generator, its electrical power $P_{EG}$ is denoted by

$$P_{EG} = T_{EG}\; w_{EG}\; \eta(T_{EG}, w_{EG}) \tag{5.17}$$

where $\eta(T_{EG}, w_{EG})$ is its efficiency given by the efficiency map shown in Figure 4.2.

Finally, based on the ICE torque and speed, a resulting fuel mass flow $\dot{m}_{fuel}$, is required. The value for $\dot{m}_{fuel}$ is obtained from the ICE consumption map that depends on ICE torque and speed. It is illustrated in Figure 4.1. Therefore, the fuel power required from the ICE is calculated as

$$P_{fuel} = \dot{m}_{fuel}\; ((T_{ice} + dw_{ice}\; \theta),\; w_{ice})\; Q_{lhv} \tag{5.18}$$

where $Q_{lhv}$ represents the fuel low heating value.

#### 5.2.2.2 Optimal Control

The energy management optimization problem can have several formulations that differ on the selected cost function, often denoted by $J$. The simplest one is the fuel mass flow consumed by the vehicle over a driving cycle of duration $t_f$ [5]. Therefore, this performance index can be written as

$$J = min_u \int_0^{t_f} \; \dot{m}_{fuel}\; (T_{req}(t), w_{req}(t), x(t), u(t))\; dt \tag{5.19}$$

subject to

$$\dot{x}(t) = \frac{dSOC}{dt} \tag{5.20}$$

$$SOC(t_0) = init\_SOC \tag{5.21}$$

$$SOC(t_f) \geq min\_SOC \tag{5.22}$$

The system state $x(t)$ is the battery SOC and $u(t) = [v(t), w(t)]$ are the power split ratios. Constraint (5.21) represents the initial value of the battery SOC and constraint (5.22) is the SOC reference for the end of the driving cycle. Therefore, the optimization problem can be formalized as the problem to reach a target SOC which, at the end of the driving cycle, is lower than the initial value, trying to minimize the ICE fuel consumption. The optimal solution to this problem requires a detailed knowledge of the future driving conditions. If the future driving conditions are perfectly known, the best efficiency way to reach a certain point can be found, therefore a fully optimal control can be implemented. It can be solved by for instance using dynamic programing approach [13]. However, this never happens in real life. The value of the battery energy depends on possible uses in the future. The fuel required for recharging depends on future opportunities to charge. The ideal battery SOC value depends on energy needs in the future. However, the decision of power split must be made "now". Therefore, some variables need to be estimated, resulting in a suboptimal solution of the stated problem.

#### 5.2.2.3 Equivalent Consumption Minimization Strategy

Dynamic programming is a powerful tool to study optimal control as well as to investigate the potential of different configurations. However, it requires long computational time and perfect look-ahead of the future driving conditions, what makes it difficult to implement in real-time energy management controller.

The Equivalent Consumption Minimization Strategy (ECMS) consists of solving the above optimization problem in a simplified way. Rather than minimizing the integral of the global fuel consumption, the problem is transformed to instead minimize a sum of power from fuel and battery at each timestep [14]. This method is derived from Pontryagin's Minimum Principle and based on (5.19) and (5.20) it can be formulated as follows [5],

$$J = min_u \int_0^{t_f} L(w(t), x(t), u(t))\, dt \tag{5.23}$$

$$\dot{x}(t) = f(w(t), x(t), u(t)) \tag{5.24}$$

where $L$ is the *Lagrangian*, $w(t)$ refers to the driving cycle variables that have to be followed and $x(t)$, $\dot{x}(t)$ and $u(t)$ are defined in previous section. The ECMS introduces a *Hamiltonian* function to be minimized at each time, that is

$$H(w(t), x(t), u(t), \lambda(t)) = L(w(t), x(t), u(t)) + \lambda(t)\ f(w(t), x(t), u(t)) \tag{5.25}$$

where

$$\dot{\lambda}(t) = \frac{-\partial H(w(t), x(t), u(t))}{\partial x(t)}. \tag{5.26}$$

The parameter $\lambda(t)$ is called *adjoint state* or *Lagrangian multiplier* and it is unknown a priori. The optimal control signal that minimize the *Hamiltonian* is given by

$$u^* = min\ (H(w(t), x(t), u(t), \lambda(t))). \tag{5.27}$$

#### 5.2.2.4 Implementing ECMS

As stated above, the ECMS consists of minimizing a sum of power from fuel and battery for each timestep while following a battery SOC reference and meeting the system constraints. The power from the battery is converted in terms of fuel consumption using an equivalence or weighing factor (approximation of the *adjoint state*). Thus, the goal of the ECMS is to minimize the *Hamiltonian* denoted by

$$H = P_{fuel}(t) + \lambda\ P_{batt}(t) \tag{5.28}$$

where $P_{fuel}(t)$ is calculated by Equation (5.18) and $P_{batt}(t)$ by

$$P_{batt}(t) = P_{EM} - P_{EG}. \tag{5.29}$$

Note that $P_{EM}$ and $P_{EG}$ are calculated by (5.16) and (5.17). Also note that, due to *QSS Toolbox* references, a positive battery power leads to a battery discharge and a negative battery power imply a battery charge. $P_{EM} > 0$ means battery energy consumption while $P_{EG} > 0$ means battery energy charge.

Therefore, the ECMS will try to find the control signals $[v, w]$ that minimize $H$, while meeting the system constraints. Note that, due to the impractical supervision of $\frac{dSOC}{dt}$, it has been replaced by $P_{batt}(t)$, which is easier to measure each timestep.

#### 5.2.2.5 Equivalence or Weighing Factor

In ECMS control strategy, the unawareness of future driving conditions is reflected in an uncertainty on the correct value of the equivalence or weighing factor. Therefore, the major difficulty of this strategy is to determine the equivalence factor. This parameter influences the system behavior as follows: if $\lambda$ is too large, the use of battery energy is penalized and the fuel consumption increases. On the other hand, if it is too small, the battery energy consumption is favored and the SOC decreases.

There are several methods to estimate $\lambda$, normally leading to a $\lambda(t)$, equivalent factor variable over the time. These methods depends on the available information about past, present and future driving conditions. One os these methods cited in [5] is applied in this thesis and it is explained below.

The basic idea is to adapt the estimation of $\lambda$ according to the instantaneous deviations of battery SOC from its reference value. A simple equation that describes this algorithm is given by

$$\lambda(t) = \lambda_0 - K_p \left(SOC(t) - SOC_{ref}\right), \tag{5.30}$$

where $\lambda_0$ is the first guess, $K_p$ a tunable factor, $SOC(t)$ the battery SOC for that timestep and $SOC_{ref}$ the battery SOC reference.

The battery SOC reference $SOC_{ref}$ is defined in [15], where the authors suggest an expression as

$$SOC_{ref}(t) = \frac{(min\_SOC - init\_SOC)}{D_{tot}}\, d(t) + init\_SOC, \tag{5.31}$$

where $D_{tot}$ is the estimation of the distance that is going to be driven and $d(t)$ is the distance covered. Note that an estimation of the total trip distance is needed. This $SOC_{ref}(t)$ value is the battery SOC reference during battery depleting mode and $min\_SOC$ is the battery SOC reference for battery sustaining mode.

Regarding the first guess $\lambda_0$, a method explained in [14] has been used. The idea is to determine two constants, $\lambda_{chg}$ and $\lambda_{dis}$, that evaluate the fuel equivalent of positive and negative electrical energy use at the end of a driving cycle. Assuming the same efficiency in the electrical path of the front and rear shaft, a simple parallel PHEV can be assumed for this test.

The simulation is run for various constant values of the control signal $v$. If the requested torque is negative it is always provided by the EM regardless the value of $v$. At the end of each run, the values of the battery energy used $E_b$ and the fuel energy used $E_f$ are collected and plotted. This has been done for driving cycle NEDC, resulting in Figure 5.5.

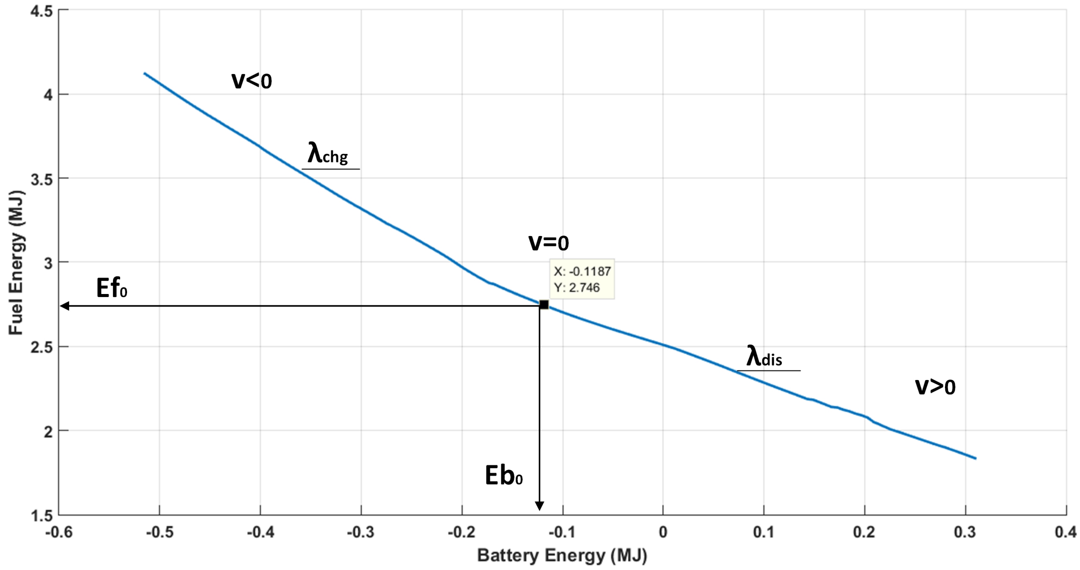


**Figure 5.5:** Plot of the dependency $E_f = f(E_b)$ for NEDC cycle.

The pure thermal case $v = 0$ is outlined in the plot. This spot separates the curve in two branches which are almost linear. The slopes of these lines are denoted by $\lambda_{chg}$ and $\lambda_{dis}$, being these values the weight of the electrical energy when charging and discharging, respectively. If $E_b$ is greater than $E_{b0}$ it means that some electrical energy has been used to drive the vehicle and therefore the fuel energy used is lower. On the other hand, if $E_b$ is lower than $E_{b0}$ it means that in addition to $E_{f0}$ some fuel has been used to store electrical energy in the battery. See [5] and [14] for further explanations of these factors. In the cited articles, it is also shown that these parameters are more or less constant for a number of standard driving cycles.

The first guess of the equivalence factor, $\lambda_0$, can be calculated as

$$\lambda_0 = \frac{\lambda_{dis} + \lambda_{chg}}{2}. \tag{5.32}$$

This value would lead to a battery sustaining mode. Therefore, if $\lambda > \lambda_0$ the use of the battery is penalized and in $\lambda < \lambda_0$ the battery will be depleted quicker. Depending on the value of $(SOC(t) - SOC_{ref})$, and thus the value of $\lambda$, the ECMS control strategy will lead to a battery depleting or battery sustaining mode.

Finally, regarding the tunable factor $K_p$, it adjusts the influence of $(SOC(t) - SOC_{ref})$ in $\lambda$ calculations. For this thesis, this parameter has been set to 0.2, as this value works well with the studied driving cycles. However, there are several methods to estimate it, and even making it variable depending on the SOC error amplitude. Moreover, there are hundreds of methods to estimate better solutions of the equivalence factor. Some of them are explained in [16], [17], [18], [19] and [20].

# 6

# Energy Efficiency Comparison

In this Chapter, both implemented energy management strategies are tested under specific driving conditions, and compared mainly in terms of fuel consumption and battery SOC behavior. The studied driving conditions are the following: driving at constant speed of 40 km/h and 100 km/h on a flat road, driving NEDC and finally driving a real life driving cycle recorded in the city of Göteborg, Sweden. The initial value of battery SOC is 80% for all simulations. The minimum SOC reference value for the ECMS strategy is 25%. For the Rule-Based strategy, the battery SOC is kept between 25% and 26% when it comes to battery sustaining mode. A SOC of 25.5% is the initial battery SOC when keeping sustaining mode since the beginning of the driving cycle.

When it comes to ECMS simulations, the $SOC_{ref}$ defined in Section 5.2.2.5 has only been used when battery sustaining mode or when battery depleting over the whole driving cycle. However, when it comes to battery depleting-sustaining mode, during battery depleting, a value of $\lambda$ lower that $\lambda_0$ has been set manually in order to achieve a battery depleting strategy that leads to a quick battery discharge.

## 6.1 Driving at Constant Speed (40 km/h)

The model has been tested driving at a constant speed of 40 km/h on a flat road during 12200 seconds, what means a total driven distance of 135.55 km.

Using the Rule-Based control strategy and a battery depleting-sustaining mode, the average fuel consumption along the trip is 1.024 l/100km and the battery SOC is shown in Figure 6.1.

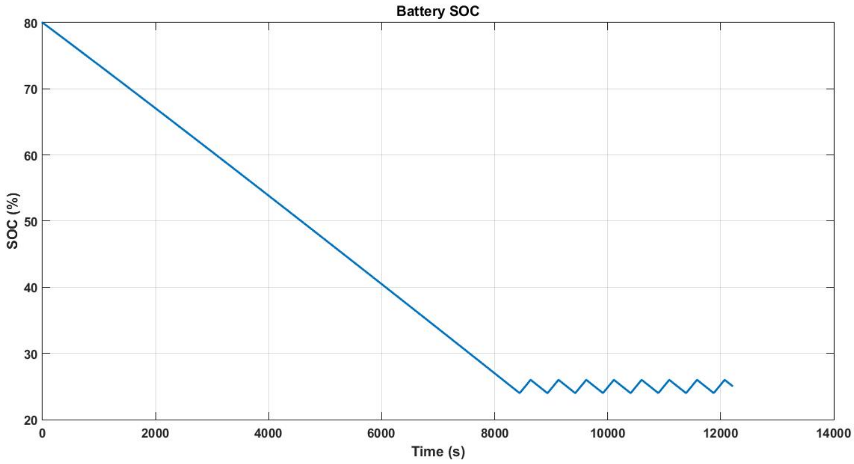


**Figure 6.1:** Battery SOC driving at constant speed of 40 km/h during 12200 s and Rule-Based battery depleting-sustaining mode.

However, if only a battery sustaining mode is taken into account, the average fuel consumption rises up to 3.199 l/100km. Figure 6.2 shows the battery SOC under this condition.

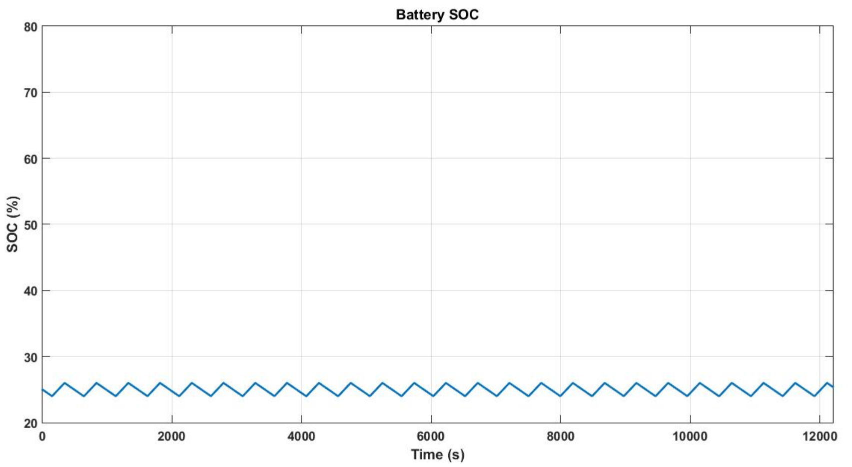


**Figure 6.2:** Battery SOC driving at constant speed of 40 km/h during 12200 s and Rule-Based battery sustaining mode.

On the other hand, if the Optimization-Based control strategy (ECMS) is used to manage the vehicle required energy, some fuel consumption improvements are achieved. Under battery depleting-sustaining mode, the fuel consumption is 0.9202 l/100km and the battery SOC is shown in Figure 6.3. It must be said that while running ECMS and during battery depleting mode, the $SOC_{ref}$ stated in Section 5.2.2.5 is not used, as the driving cycle is assumed not to be known. However, in Section 6.5, assuming a complete knowledge about future driving conditions some simulations are done and the results explained.

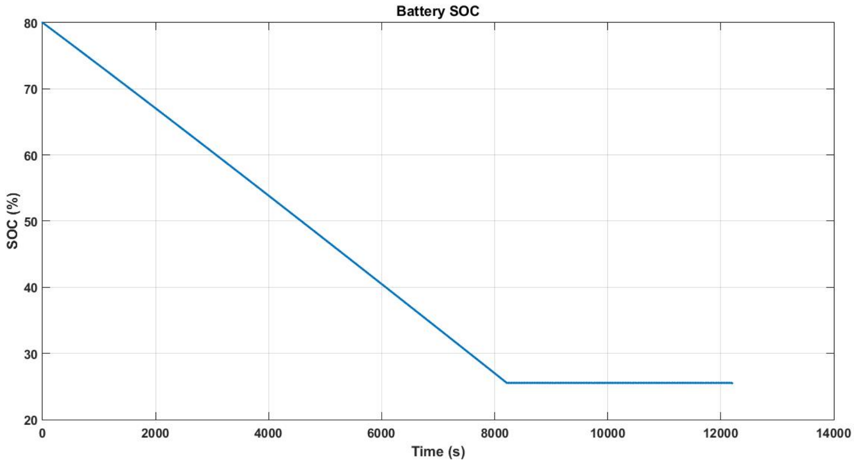


**Figure 6.3:** Battery SOC driving at constant speed of 40 km/h during 12200 s and Optimization-Based battery depleting-sustaining mode.

Under a battery sustaining mode, the fuel consumption is 2.944 l/100km and battery SOC is plotted in Figure 6.4.

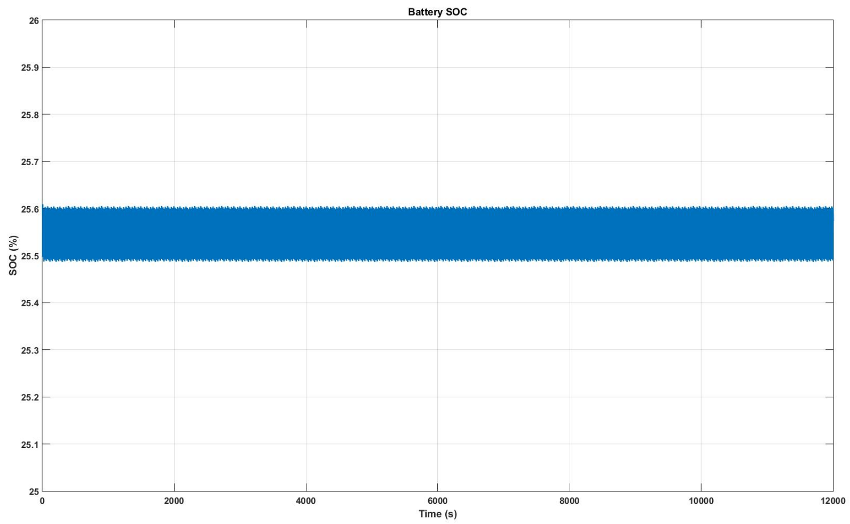


**Figure 6.4:** Battery SOC driving at constant speed of 40 km/h during 12200 s and Optimization-Based battery sustaining mode.

## 6.2 Driving at Constant Speed (100 km/h)

The model has also been tested driving at a constant speed of 100 km/h on a flat road during 12200 seconds, which results in a total driven distance of 338.9 km.

Being the Rule-Based control strategy the energy management method and the battery depleting-sustaining mode, the average fuel consumption along the trip is 5.537 l/100km and the battery SOC is shown in Figure 6.5.

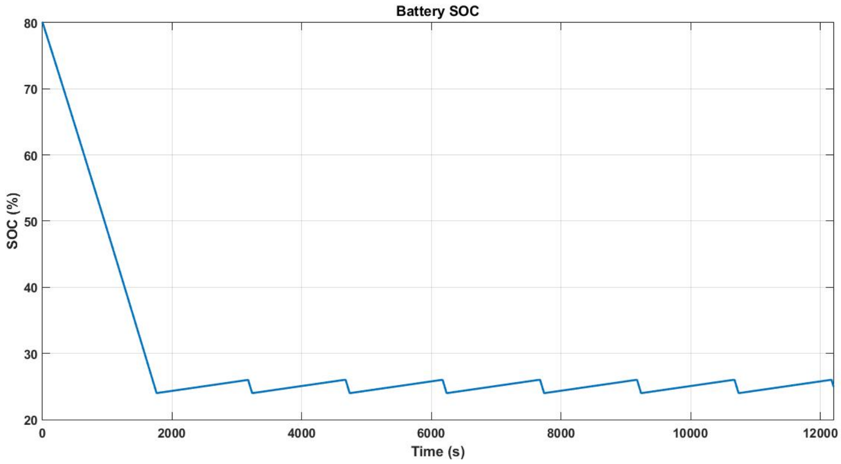


**Figure 6.5:** Battery SOC driving at constant speed of 100 km/h during 12200 s and Rule-Based battery depleting-sustaining mode.

With the same energy management strategy but with a battery sustaining mode, the fuel consumption is 6.435 l/100km and battery SOC is plotted in Figure 6.6.

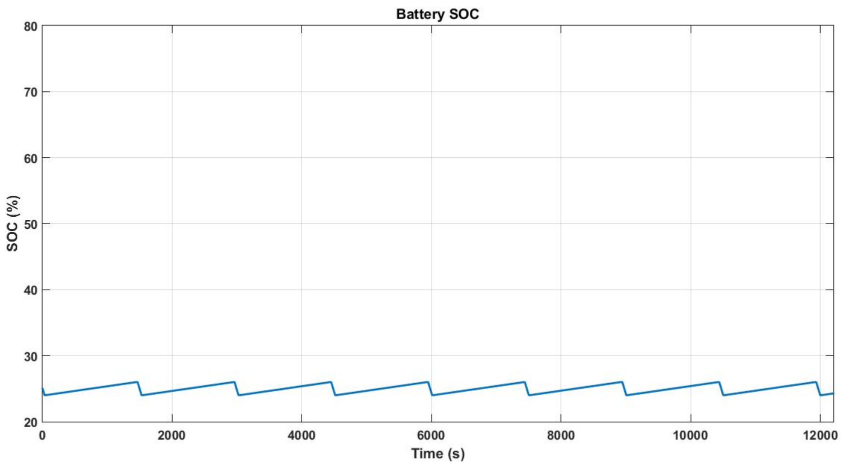


**Figure 6.6:** Battery SOC driving at constant speed of 100 km/h during 12200 s and Rule-Based battery depleting-sustaining mode.

If the Optimization-Based control strategy (ECMS) is used to manage the energy, some fuel consumption improvements are achieved. Under battery depleting-sustaining mode, the fuel consumption is 5.081/100km and the battery SOC is shown in Figure 6.7. As stated in Section 6.2, while running ECMS and during battery depleting mode, the $SOC_{ref}$ stated in Section 5.2.2.5 is not used, as the driving cycle is assumed to be unknown.

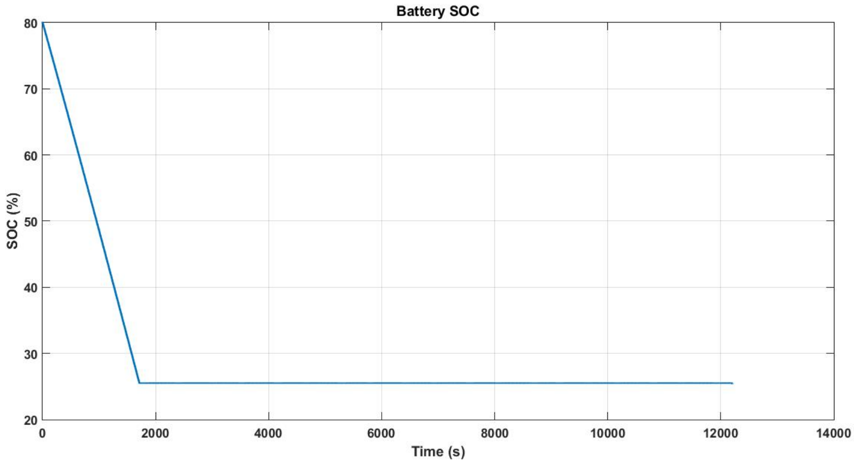


**Figure 6.7:** Battery SOC driving at constant speed of 100 km/h during 12200 s and Optimization-Based battery depleting-sustaining mode.

Using a battery sustaining mode, the fuel consumption is 5.909 l/100km and battery SOC is plotted in Figure 6.8.

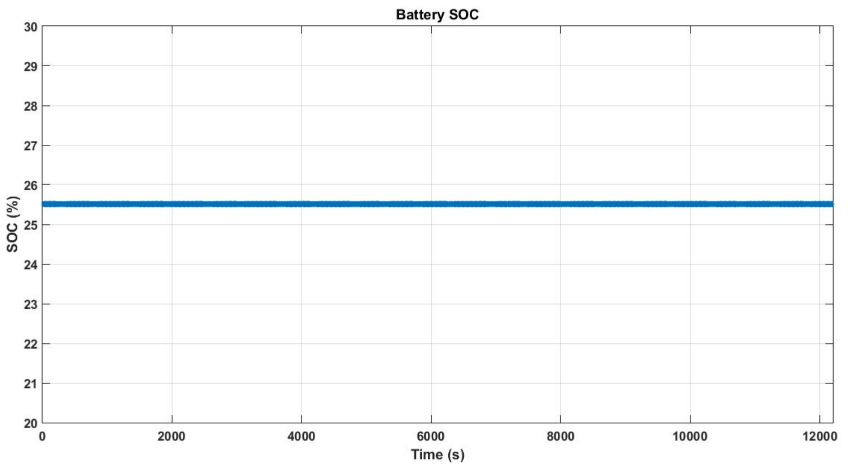


**Figure 6.8:** Battery SOC driving at constant speed of 100 km/h during 12200 s and Optimization-Based battery sustaining mode.

## 6.3 Driving NEDC

NEDC, also known as MVEG-95, is the official cycle to standardize pollutant emissions and vehicle autonomy in Europe. as it is a standard driving cycle, it allows to compare the pollutant emissions and fuel economy of different vehicles on the same basis. That is why the studied model has also been tested running NEDC ten times consecutively.

With the Rule-Base control strategy and a battery depleting-sustaining mode, the vehicle fuel consumption is 2.539 l/100km and the battery SOC is shown in Figure

6.9.

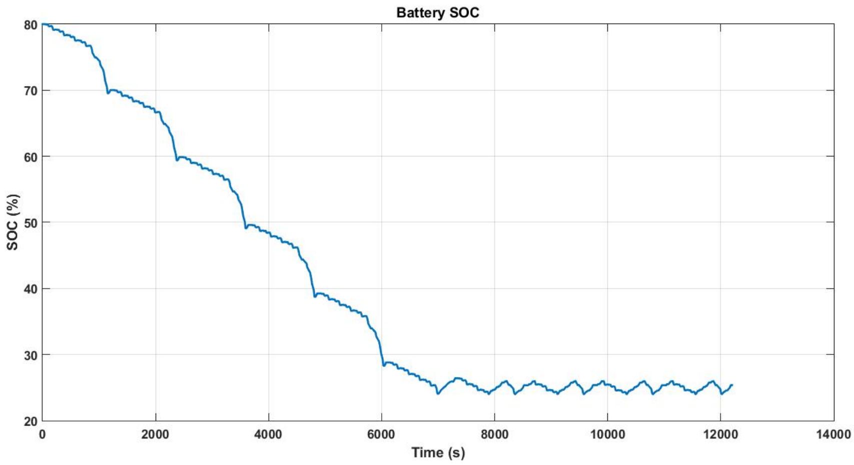


**Figure 6.9:** Battery SOC driving NEDC 10 times and Rule-Based battery depleting-sustaining mode.

However, if a battery sustaining mode is kept from the beginning of the driving cycle, the fuel consumption increases up to 4.96 l/100km. The battery SOC is plotted in Figure 6.10.

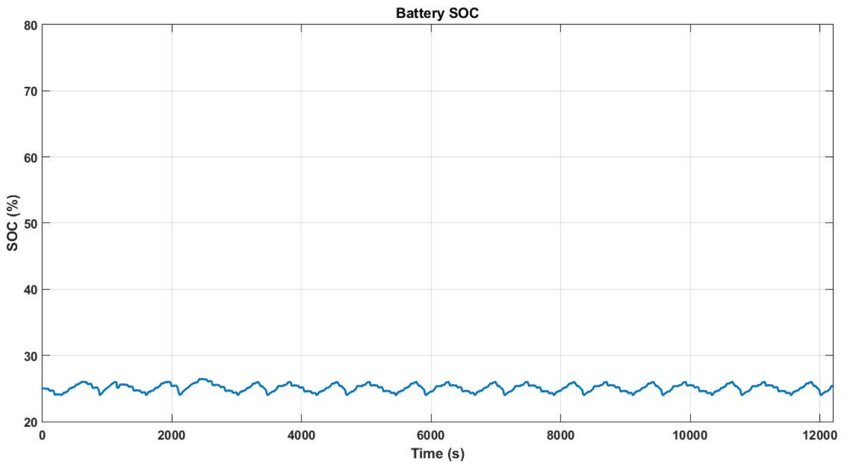


**Figure 6.10:** Battery SOC driving NEDC 10 times and Rule-Based battery sustaining mode.

It is possible to reduce the fuel consumption if the Optimization-Based strategy is used. With a battery depleting-sustaining mode the fuel consumption is 2.04 l/100km and the battery SOC is shown in Figure 6.11.

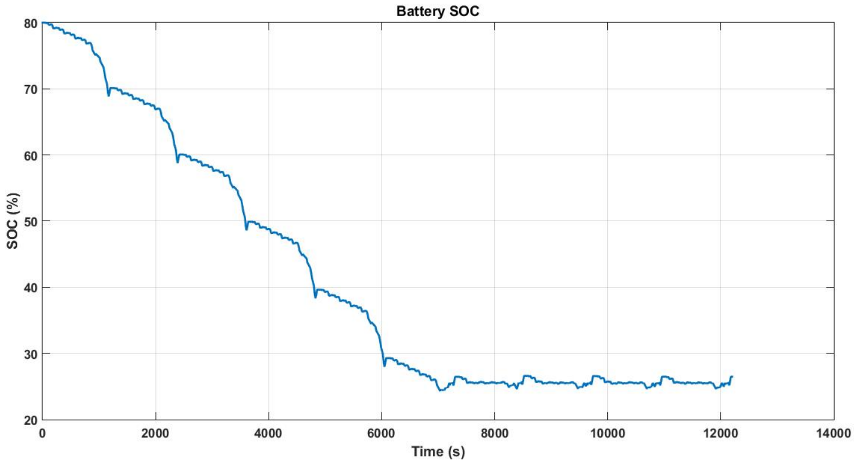


**Figure 6.11:** Battery SOC driving NEDC 10 times and Optimization-Based battery sustaining mode.

If only a battery sustaining mode is taken into account, the fuel consumption increases up to 4.499 l/100km. The corresponding battery SOC is plotted in Figure 6.12.

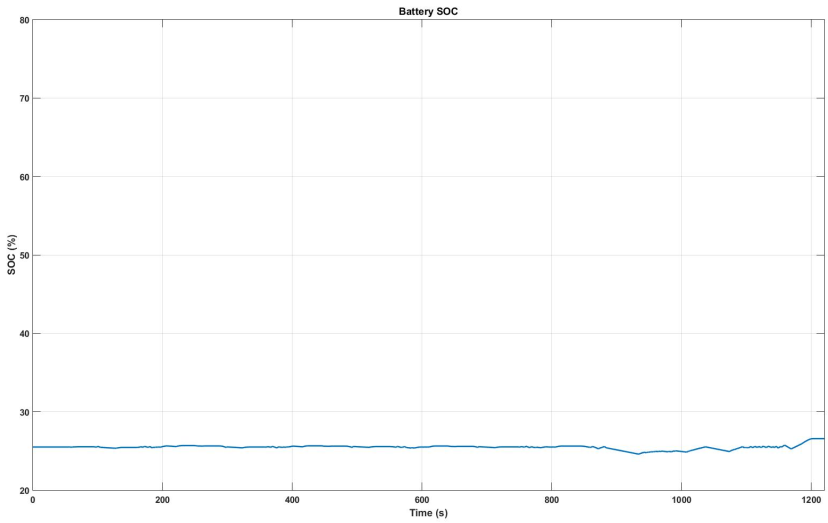


**Figure 6.12:** Battery SOC driving NEDC 10 times and Optimization-Based battery sustaining mode.

## 6.4 Driving a Real Life Cycle

The model has been also tested running a real life driving cycle recorded in the city of Göteborg, Sweden. The vehicle speed profile of this cycle is shown in Figure 6.13.

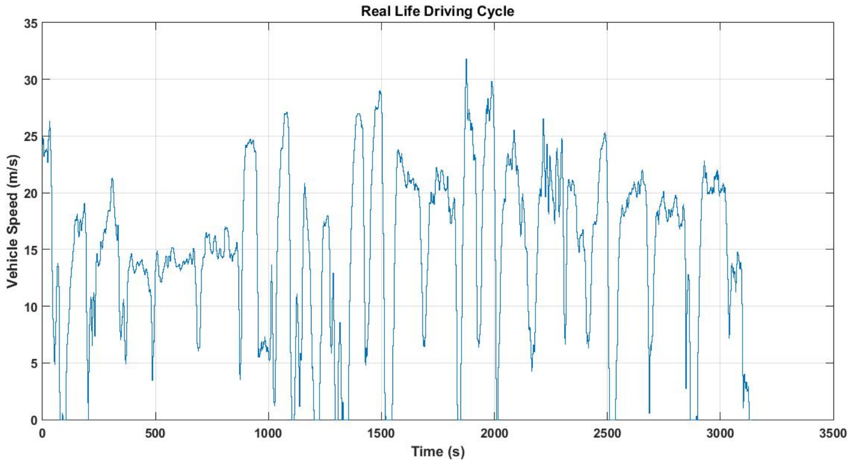


**Figure 6.13:** Vehicle speed profile of a real life driving cycle recorded in the city of Göteborg, Sweden.

The driving cycle has been run ten times consecutively using both energy management control strategies. The results are discussed below.

First, working with the Ruled-Based strategy and adopting a battery depleting.sustaining mode, the vehicle fuel consumption is 5.142 l/100km and its battery SOC profile is plotted in Figure 6.14.

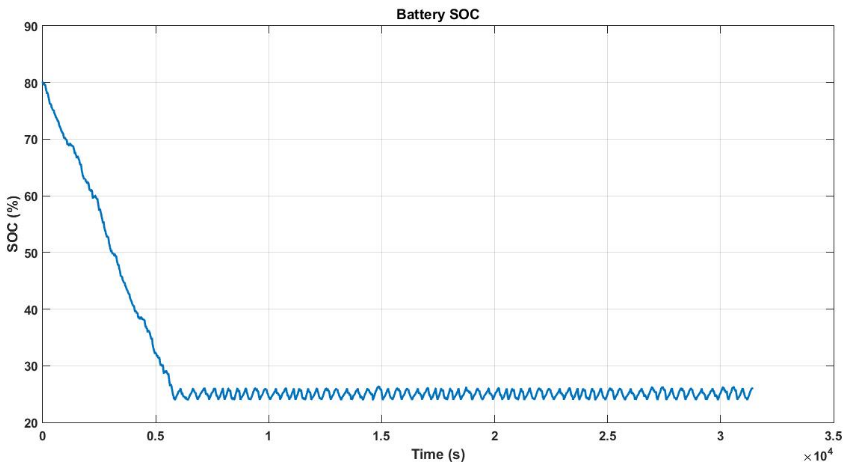


**Figure 6.14:** Battery SOC driving a real life cycle with Rule-Based and battery depleting-sustaining mode.

If a battery sustaining mode applied since the beginning of the driving cycle, the fuel consumption increases up to 5.677 l/100km. The corresponding battery SOC is shown in Figure 6.15.

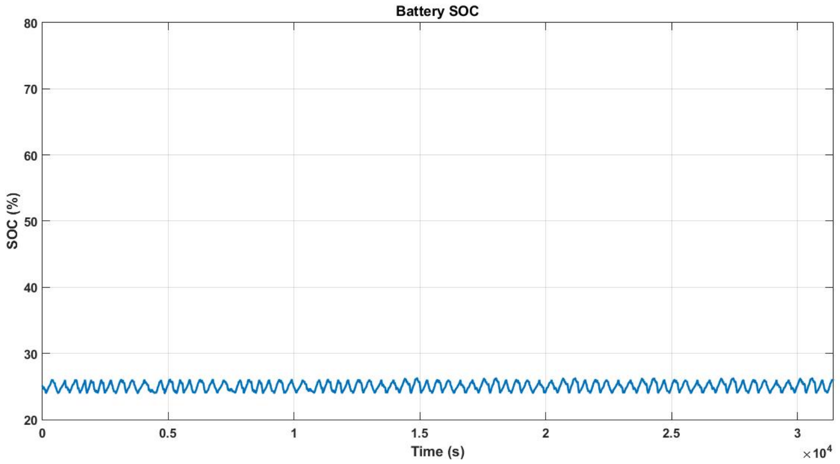


**Figure 6.15:** Battery SOC driving a real life cycle with Rule-Based and battery sustaining mode.

On the other hand, the following results demonstrate how operating with the Optimization-Based strategy (ECMS) implies a fuel consumption reduction. If a battery depleting-sustaining mode is established, the vehicle fuel consumption is 4.407 l/100km and the corresponding battery SOC profile is shown in Figure 6.16.

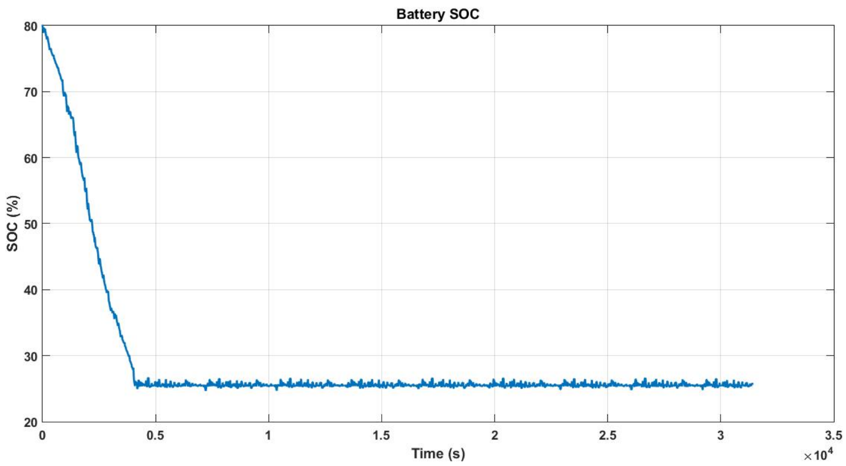


**Figure 6.16:** Battery SOC driving a real life cycle with Optimization-Based and battery depleting-sustaining mode.

If the battery sustaining mode is set since the beginning of the driving cycle, the fuel consumption increases up to 4.918 l/100km. The battery SOC profile is displayed in Figure 6.17.

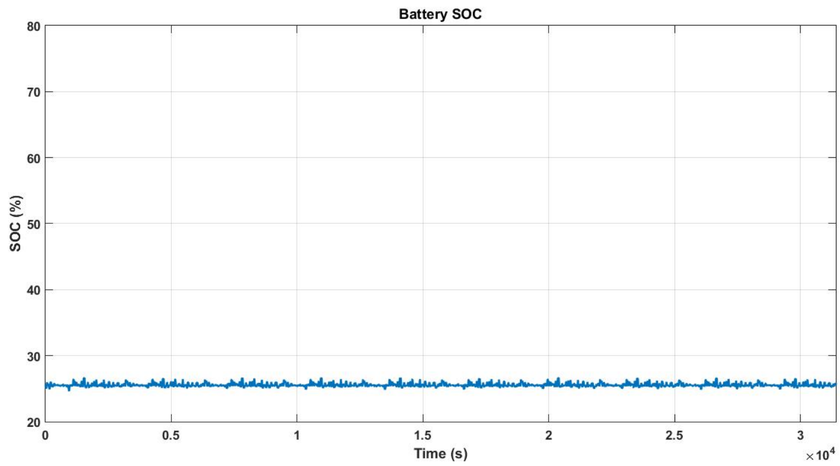


**Figure 6.17:** Battery SOC driving a real life cycle with Optimization-Based and battery sustaining mode.

## 6.5 ECMS with Previous Knowledge of Future Driving Conditions

As mentioned in Section 5.2.2.2, the optimal solution of the optimization problem can be found if the future driving conditions are perfectly known a priori.

Several simulations has been run in order to calculate the corresponding $\lambda_0$ that leads to a battery depleting across the whole driving cycle, i.e. no battery sustaining mode allowed. This calculation has been done with trial and error method, varying the value of $\lambda_0$ until the right battery SOC profile is achieved. Of course this method does not work in real life. However, all the available information about the future driving conditions could be added to a proper regulator that sets the right value of $\lambda$ each timestep, in order to get the desired battery discharging profile. The results achieved with the simple simulations explained above are shown below.

Driving at 40 km/h during 12200 seconds the fuel consumption is 0.9697 l/100km and the battery SOC profile is plotted in Figure 6.18.

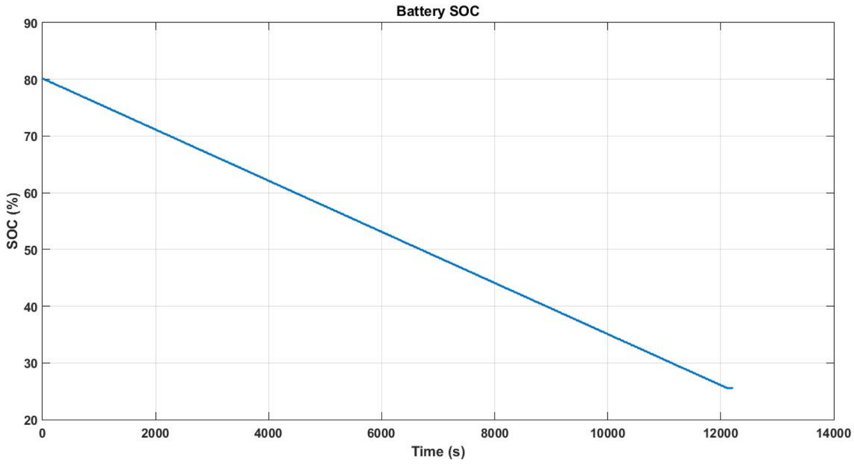


**Figure 6.18:** Battery SOC driving at 40 km/h during 12200 s. Optimization-Based strategy and battery depleting across the whole driving cycle.

For a constant speed of 100 km/h during 12200 seconds the fuel consumption is 5.157 l/100km and the battery SOC profile is shown in Figure 6.19.

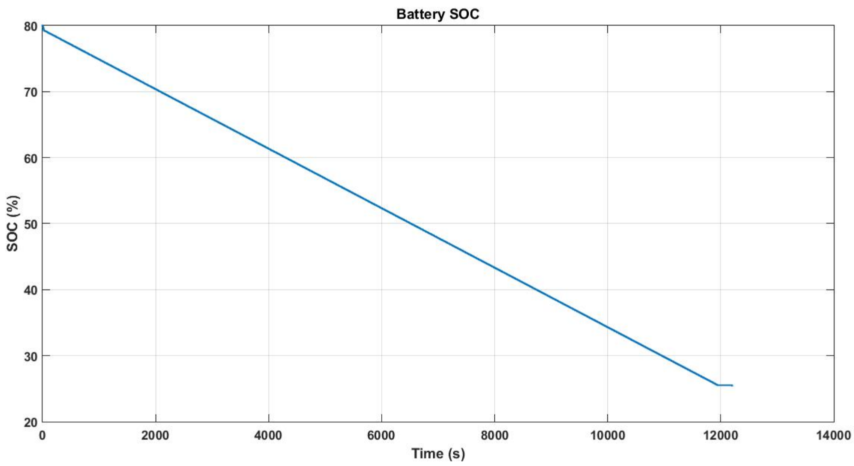


**Figure 6.19:** Battery SOC driving at 100 km/h during 12200 s. Optimization-Based strategy and battery depleting across the whole driving cycle.

NEDC run 10 times gives a fuel consumption of 1.88 l/100km and the battery SOC profile plotted in Figure 6.20.

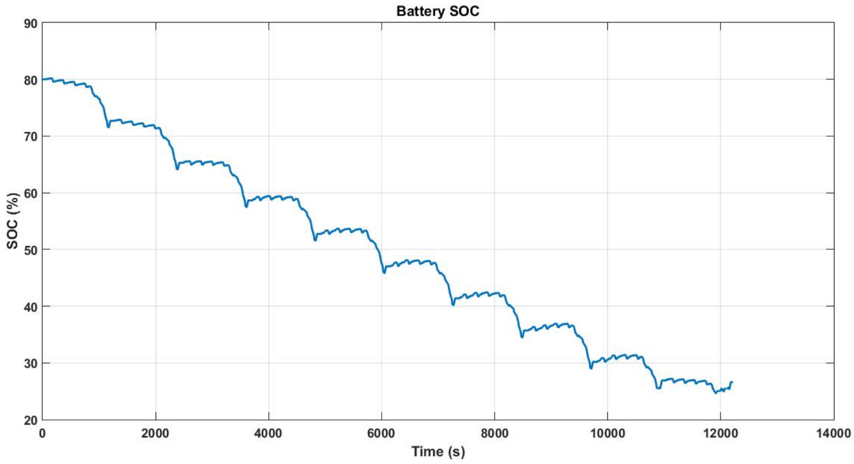


**Figure 6.20:** Battery SOC driving at 100 km/h during 12200 s. Optimization-Based strategy and battery depleting across the whole driving cycle.

Finally, the real life driving cycle displays a fuel consumption of 4.904 l/100km and the battery SOC profile of Figure 6.21.

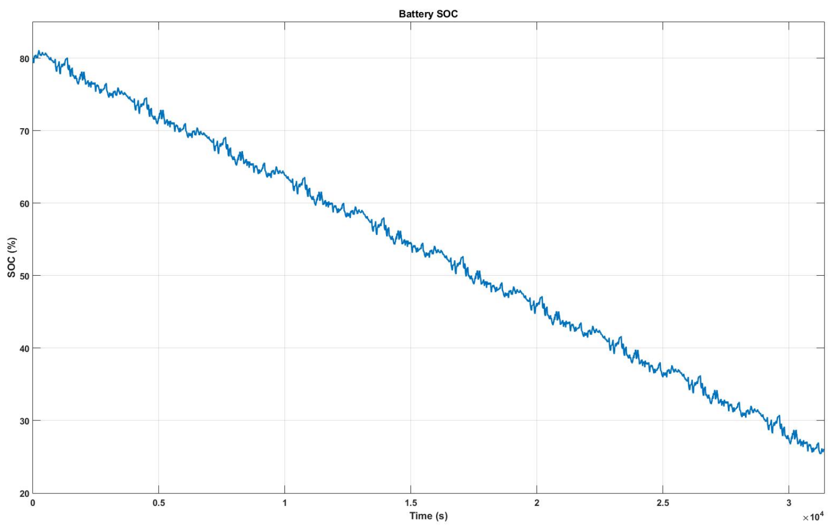


**Figure 6.21:** Battery SOC driving a real life cycle recorded in Göteborg, Sweden. Optimization-Based strategy and battery depleting across the whole driving cycle.

## 6.6 Fuel Consumption Comparison

Table 6.1 collects the fuel consumptions stated in the previous sections. According to the last row, it can be seen that the Equivalent Consumption Minimization Strategy leads to significant fuel reductions in all the studied situations.

**Table 6.1:** Fuel consumption comparison. DS: battery depleting-sustaining mode. S: battery sustaining mode.

| Fuel Consumption (l/100km) | 40 km/h | | 100 km/h | | NEDC | | Real Life Driving Cycle | |
|---|---|---|---|---|---|---|---|---|
| | DS | S | DS | S | DS | S | DS | S |
| **Rule-Based Strategy** | 1.024 | 3.199 | 5.537 | 6.435 | 2.539 | 4.960 | 5.142 | 5.677 |
| **ECMS** | 0.9202 | 2.944 | 5.081 | 5.909 | 2.040 | 4.499 | 4.407 | 4.918 |
| **% of fuel change (ECMS over RB)** | **-10.13** | **-7.97** | **-8.23** | **-8.17** | **-19.65** | **-9.29** | **-14.29** | **-13.37** |

Table 6.2 collects the fuel consumption using ECMS with battery discharge over the whole driving cycle for all studied driving cycles. The last row of this table shows the fuel reduction of this last control strategy in comparison with the battery depleting-sustaining mode. It can be noticed that only in one of the studied cases a better fuel consumption is achieved through this battery discharging mode.

**Table 6.2:** Fuel consumption using ECMS with battery discharge over the whole driving cycle

| Fuel Consumption (l/100km) | 40 km/h | 100 km/h | NEDC | Real Life Driving Cycle |
|---|---|---|---|---|
| **ECMS with battery discharge over the whole driving cycle** | 0.9697 | 5.157 | 1.88 | 4.904 |
| **% of fuel change (ECMS with battery discharge over the whole driving cycle vs ECMS with battery depleting-sustaining mode)** | **+ 5.38** | **+ 1.48** | **- 7.80** | **+ 11.35** |

## 6.7 Further Analysis on NEDC Driving Cycle

Further analysis has been done in order to analyze the boundaries of the model, which are the pure ICE mode and pure EV mode. The model has been run under NEDC driving conditions for pure ICE mode, pure EV mode, hybrid mode with battery depleting strategy and hybrid mode with battery sustaining strategy. Table 6.3 shows the fuel and battery energy consumption of the previous cases. One can clearly notice the fuel saving potential of hybridization. However, these results should make someone to think about the way the battery charging energy is obtained. If most of the electricity is generated from fossil fuels, the sustainability advantages of hybridizations might go down.

**Table 6.3:** Fuel and battery energy consumption of the vehicle running NEDC for pure ICE, pure EV and hybrid mode.

| NEDC | Fuel Consumption (l / 100 km) | Fuel Energy Content (kWh) | Battery Energy Consumption (kWh) |
|---|---|---|---|
| **Pure ICE** | 6.418 | 5.187 | -0.296 (regenerative braking) |
| **Pure EV** | 0 | 0 | 1.406 |
| **Hybrid Battery Depleting (ECMS)** | 0.086 | 0.069 | 1.211 |
| **Hybrid Battery Sustaining (ECMS)** | 4.187 | 3.385 | -0.0132 (difference between initial and final SOC) |

As it can be noticed from Table 6.3, the amount of electric energy needed to propel the vehicle on pure EV mode corresponds to a 27.11 % of the fuel energy needed to propel the vehicle on pure ICE mode.

If a fossil liquid fuel is burned in a power plant in order to produced electricity, the total efficiency (from fuel energy content to final user electric energy) could be from 20 % to 40 %. Therefore, if the electric energy needed to propel the vehicle on pure EV is obtained from a similar liquid fuel the amount of fuel needed would be the same as the one needed to propel the vehicle on pure ICE mode.

In conclusion, electric propulsion could not be such a beneficial alternative to traditional fuel propulsion while most of the electricity is not obtained from renewable sources.

# 7

# Sensitivity Analysis

In this chapter, two cases are analyzed. First, the equivalence factor $\lambda_0$ that leads to a battery sustaining SOC is calculated for different values of the internal battery resistance. Second, a new PHEV model, where the electric generator is removed, is compared with the original model in terms of fuel consumption.

## 7.1 Influence of Battery Internal Resistance on Equivalence Factor

Multiple phenomena related to cycling and time cause battery aging. The battery degradation increases with the depth of discharge, frequency of cycling, elevated voltages and currents, high temperatures, etc. The effect of degradation is an increase of battery internal resistance and a reduction in capacity. According to [21], a maximum increase of 20% in battery resistance over 10 years would be something acceptable.

If the battery internal resistance increases, higher battery loses are expected. Therefore, as the equivalence factor $\lambda$ depends on battery energy consumption, a variation of this parameter over the battery resistance growth is expected. Thus, several simulations have been done in order to correlate the value of $\lambda_0$, the equivalence factor that leads to a battery sustaining SOC obtained in Section 5.2.2.5 for NEDC cycle, with the battery internal resistance. Figure 7.1 shows this correlation.

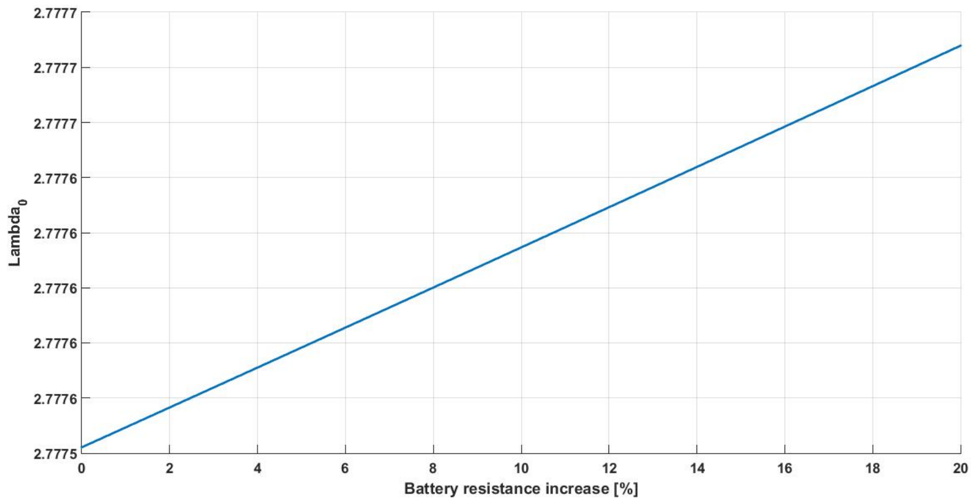


**Figure 7.1:** Value of $\lambda_0$ as a function of battery internal resistance increase.

As it can be observed from Figure 7.1, the value of $\lambda_0$ varies a 0.001% over a 20% variation in battery resistance, which is a non symbolic fluctuation. It is possible to conclude that once a $\lambda_0$ is estimated for a certain driving cycle, it can remain constant for the life cycle of the vehicle.

## 7.2 Removing the Electric Generator

The role of the electric generator in the studied model is to charge the battery with extra torque provided by the ICE. Another approach for a PHEV is the same configuration but without the generator, i.e. the electric motor would also use some torque from the ICE to charge the battery. An advantage of this new PHEV topology is that the losses in the belt transmission between the ICE and the EG are avoided. However, the vehicle cannot be propelled by the EM at the same time as the battery is charged, whereas in the original model it is possible because of the EG.

In order to quantify these advantages and disadvantages, the electric generator is removed and the fuel consumption studied and compared to the one from the PHEV with generator. For this test, ECMS strategy has been used, being the one that leads to better results. Moreover, the model has been studied under NEDC driving conditions.

First, the model is run under a battery depleting-sustaining mode, achieving a fuel consumption of 2.392 l/100km and a battery SOC profile plotted in Figure 7.2.

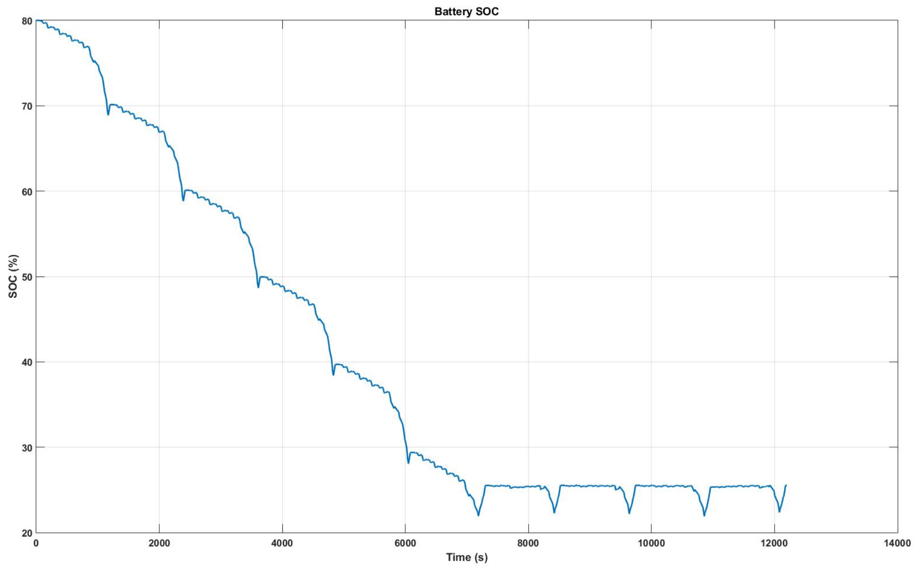


**Figure 7.2:** Battery SOC of a PHEV without generator driving NEDC 10 times. ECMS control strategy and battery depleting-sustaining mode.

Second, assuming only a battery sustaining mode, the fuel consumption increases up to 5.115 l/100km and the battery SOC profile is shown in Figure 7.3.

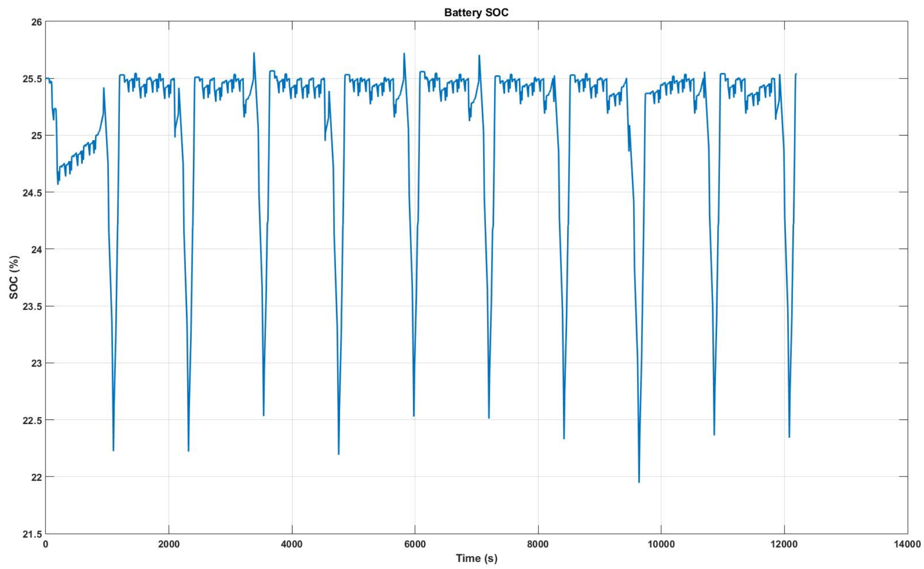


**Figure 7.3:** Battery SOC of a PHEV without generator driving NEDC 10 times. ECMS control strategy and battery sustaining mode.

Third, with a battery depleting over the whole driving cycle the fuel consumption is 3.172 l/100km. Figure 7.4 shows the battery SOC profile for this last mode.

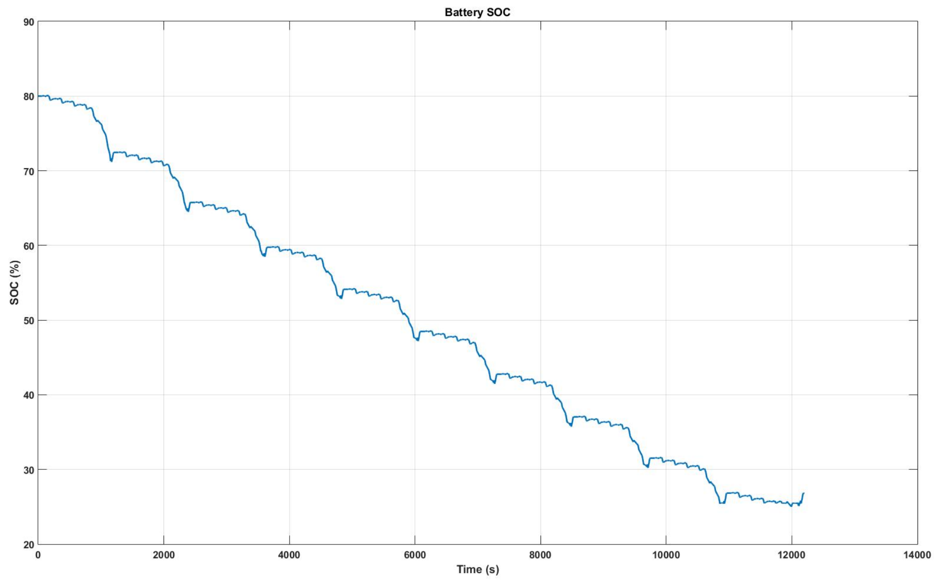


**Figure 7.4:** Battery SOC of a PHEV without generator driving NEDC 10 times. ECMS control strategy and battery depleting over the whole driving cycle.

Table 7.1 collects the previous fuel consumptions and they are compared with the results from a PHEV with generator. It is shown that the fuel consumption significantly increases due to the generator removal. Moreover, in the above SOC profiles, it is shown that the battery SOC suffers more variations from its reference value (sustaining mode) when the generator is removed.

**Table 7.1:** Fuel consumption comparison of series-parallel PHEV vs parallel PHEV running NEDC 10 times under different battery discharging modes. DS: battery depleting-sustaining mode. S: battery sustaining mode.

| **Fuel Consumption (l/100km)** | **NEDC 10 times** | | |
|---|---|---|---|
| | **DS** | **S** | **Battery depleting over the whole drive cycle** |
| **Series-Parallel PHEV** | 2.040 | 4.499 | 1.88 |
| **Parallel PHEV (no generator)** | 2.392 | 5.115 | 3.172 |
| **% of fuel change (Parallel PHEV over Series-Parallel PHEV)** | **+ 17.25 %** | **+ 13.70 %** | **+ 68.72 %** |

The reason why the fuel consumption increases is because in a simple parallel PHEV if the vehicle has to be propelled by the ICE, the operating point is fixed whereas in a series-parallel PHEV, that ICE operating point can be move up to a better efficiency point and charge the battery with the ICE torque while propelling the vehicle with the EM. Moreover, in the series-parallel PHEV the vehicle can be propelled on electricity at the same time the battery is being charged. Thus, a better SOC control and lower fuel consumptions are achieved.

In an attempt to try to reduce the fuel consumption of the PHEV without generator, another possible parameter configuration has been tested. In this case, the minimum SOC reference value is increased to 30% and the equivalence or weighing factor $\lambda$ is relaxed ($\lambda_0 = 2$ and $K_p = 0.1$) in order to allow higher SOC variations during battery sustaining mode, but keeping in mind that the battery SOC cannot reach a value of 20% as it would be harmful for the battery. Table 7.2 shows that even with this strategy the fuel consumption increases due to the generator removal. It is a bit lower than the previous case but it could be due to the larger SOC variation in the battery sustaining mode. However, it seems that changing the available SOC window and the way $\lambda$ is calculated, better results could be achieved with a simple parallel PHEV without generator, but further analysis would be needed.

**Table 7.2:** Fuel consumption comparison of series-parallel PHEV vs parallel PHEV running NEDC 10 times under different battery discharging modes. DS: battery depleting-sustaining mode. S: battery sustaining mode. (Minimum SOC reference value = 30%, $\lambda_0 = 2$ and $K_p = 0.1$)

| **Fuel Consumption (l/100km)** | **NEDC 10 times** | |
|---|---|---|
| | **DS** | **S** |
| **Series-Parallel PHEV** | 2.040 | 4.499 |
| **Parallel PHEV (min SOC = 30% and $\lambda$ relaxed)** | 2.385 | 5.104 |
| **% of fuel change (Parallel PHEV over Series-Parallel PHEV)** | **+ 16.91 %** | **+ 13.44%** |

# 8

# Conclusions

In this chapter, the conclusions of this master thesis are summarized. Moreover, few future work recommendations are suggested in order to continue this line of research.

## 8.1 Results

The main results of this thesis can be summarized with the following conclusions:

1. A model of a series-parallel plug-in hybrid electric vehicle has been built using *Matlab Simulink* and its toolbox *QSS*.

2. A smart gearbox controller that selects the best gear each timestep has been included in order to control the automatic gearbox that connects the ICE with the front shaft.

3. Two different energy management strategies have been implemented. First, a rule-based strategy that relies on intuition and experience-based rules, which are the most common control strategies for PHEV nowadays. Second, an optimization-based algorithm that minimizes the sum of fuel and battery power each timestep has been introduced as an alternative to classic control approaches.

4. Both energy management strategies have been tested on the build model under different driving conditions: constant speeds of 40 and 100 km/h, NEDC and a real life driving cycle recorded in the city of Göteborg, Sweden. Moreover, different battery discharge strategies have been compared.

5. From the results in Chapter 6, it can be seen that the control strategies work as expected, allowing the three different analyzed battery discharge strategies. From the results in Table 6.1, it can be concluded that the optimization-based algorithm achieves better results when it comes to fuel consumption under all studied cases. Compared to the rule-based strategy, the optimization-based strategy reduces the fuel consumption in the range of 8-20 % depending on the driving cycle and battery discharge strategy.

6. For a battery discharge over the whole driving cycle, the fuel consumption nor-

mally increases compared to a depleting-sustaining mode. Only under NEDC driving conditions the fuel consumption decreases. These results were the opposite as expected, but perhaps it could be improve if a better $\lambda$ regulator is introduced.

7. The influence of the battery internal resistance on the equivalence factor $\lambda$ has also been analyzed. A variation of $\lambda_0$ over a 20 % increase of battery resistance is barely 0.001 %. Therefore, it can be concluded that the battery internal resistance does not affect the estimation of $\lambda_0$.

8. Finally, a PHEV model without generator has been modeled in order to analyze the influence of the generator on fuel consumption. The fuel consumption significantly increases due to the generator removal in all studied cases. Furthermore, the battery SOC profiles show higher variations from its reference value. Thus, one can conclude that with two electric machines a better battery discharge profile is achieved, as the vehicle can be propelled on electricity at the same time that the battery is being charged.

## 8.2 Future Work

Some future work suggestion are pointed out below:

1. Regarding the vehicle model many improvements can be done in order to make it more real. For instance, real life ICE consumption map, EM and EG efficiency maps could be added. Moreover, auxiliary loads should be included.

2. Due to *QSS* electric generator model, the EG used in this thesis cannot help to boost the vehicle. However, a generator model with working areas in both quadrants could be added for future analysis.

3. With respect to the gearbox controller, the gear is shifted every timestep if it provides better fuel consumption. In real life a gearbox cannot shift every second so some improvements should be done regarding this issue.

4. Something similar to the previous issue is that the ICE can be turned on or off every timestep. An improvement should be added in order to avoid too many ICE starts.

5. With regards to the rule-based strategy, the minimum ICE speed and torque could be increased to analyze the influence of these rules on fuel consumption.

6. The most interesting future work is related to the estimation of the equivalence factor $\lambda$ in the ECMS strategy. In this thesis, a simple method to estimate this parameter has been used and it is explained in Section 5.2.2.5. However, there are hundreds of methods to estimate better solutions of the equivalence factor,

especially if future driving conditions are known a priori. Moreover, a better regulator that sets the right value of $\lambda$ each timestep should be investigated.

# Bibliography

[1] Europe 2020 targets: http://ec.europa.eu/europe2020/targets/eu-targets/ [Retrieved 2016-04-03]

[2] A. Y. Saber and G. K. Venayagamoorthy, "Plug-in Vehicles and Renewable Energy Sources for Cost and Emission Reductions," in IEEE Transactions on Industrial Electronics, vol. 58, no. 4, pp. 1229-1238, April 2011

[3] Electric Drive Sales Dashboard: http://electricdrive.org/index.php?ht=d/sp/i/20952/pid/20952 [Retrieved 2016-04-03]

[4] A. Amstutz L. Guzzella. The QSS Toolbox Manual, 2005.

[5] Lino Guzzella, Antonio Sciarretta, "Vehicle Propulsion Systems: Introduction to Modeling and Optimization". Springer, third edition.

[6] Insup Kim; Hyunsup Kim, "Configuration analysis of plug-in hybrid systems using global optimization", in Electric Vehicle Symposium and Exhibition (EVS27), 2013 World , vol., no., pp.1-14, 17-20 Nov. 2013.

[7] A. Da Costa et. Al., "Fuel Consumption Potential of Different Plug-in Hybrid Vehicle Architectures in the European and American Contexts", EVS26, Los Angeles, California, May 6-9, 2012.

[8] Chau K., Wong Y., 2002. "Overview of power management in hybrid electric vehicles. Energy Conversation and Management", Volume 43, Issue 15, October 2002, Pages 1953-1968

[9] Salmasi, F.R., "Control Strategies for Hybrid Electric Vehicles: Evolution, Classification, Comparison, and Future Trends," in Vehicular Technology, IEEE Transactions on , vol.56, no.5, pp.2393-2404, Sept. 2007

[10] O. Tremblay, Louis-A. Dessaint, Abdel-Illah Dekkiche, "A Generic Battery Model for the Dynamic Simulation of Hybrid Electric Vehicles," in Vehicle Power and Propulsion Conference, 2007. VPPC 2007. IEEE , vol., no., pp.284-289, 9-12 Sept. 2007

[11] H. Banvait, S. Anwar and Y. Chen, "A rule-based energy management strategy for Plug-in Hybrid Electric Vehicle (PHEV)," American Control Conference, 2009. ACC '09., St. Louis, MO, 2009, pp. 3938-3943.

[12] A. E. Trippe, R. Arunachala, T. Massier, A. Jossen and T. Hamacher, "Charging optimization of battery electric vehicles including cycle battery aging," Innovative Smart Grid Technologies Conference Europe (ISGT-Europe), 2014 IEEE PES, Istanbul, 2014, pp. 1-6.

[13] H. Banvait, J. Hu and Y. Chen, "Design of energy management system of Plug-in Hybrid Electric Vehicle using hybrid systems," American Control Conference (ACC), 2015, Chicago, IL, 2015, pp. 1339-1344.

[14] A. Sciarretta, M. Back and L. Guzzella, "Optimal control of parallel hybrid electric vehicles," in IEEE Transactions on Control Systems Technology, vol. 12, no. 3, pp. 352-363, May 2004.

[15] Tulpule, P., Marano, V. and Rizzoni, G. (2010) "Energy management for plug-in hybrid electric vehicles using equivalent consumption minimisation strategy", Int. J. Electric and Hybrid Vehicles, Vol. 2, No. 4, pp.329–350.

[16] Jeon, S.I., Jo, S.T., Park, Y.I., Lee, J.M. "Multi-mode driving control of a parallel hybrid electric vehicle using driving pattern recognition". Transactions of the ASME, Journal of Dynamic Systems, Measurement, and Control 124, 141–149.

[17] Kessels, J.T.B.A., Koot, M.W.T., van den Bosch, P.P.J., Kok, D.B. "Online energy management for hybrid electric vehicles". IEEE Transactions on Vehicular Technology 57(6), 3428–3440.

[18] Salman, M., Chang, M.F., Chen, J.S. "Predictive energy management strategies for hybrid vehicles". In: Proc. of the IEEE Vehicle Power and Propulsion Conference, Chicago, IL.

[19] C. Zhang and A. Vahid, "Real-time optimal control of plug-in hybrid vehicles with trip preview," American Control Conference (ACC), 2010, Baltimore, MD, 2010, pp. 6917-6922.

[20] Fredrik O. Johansson, Ali Rabiei. "Energy Management in a hybrid vehicle using predicted road slope information. Master of science thesis, Chalmers University of Technology; Department of Energy and Environment. Göteborg, Sweden.

[21] K. Smith, M. Earleywine, E. Wood, J. Neubauer, and A. Pesaran, "Comparison of plug-in hybrid electric vehicle battery life across geographies and drive cycles, " SAE Technical Paper, 2012.